PROTON-GAMMA ANGULAR CORRELATIONS IN THE $C^{12}(d,p)C^{13}$ REACTION AT LOW ENERGIES

by

Thomas Sidney Katman

Department of Physics
Duke University

Date: _____

Approved:

_____
Robert M. Williamson, Supervisor

_____

_____

_____

_____

A dissertation submitted in partial fulfillment of the requirements for the degree of Doctor of Philosophy in the Department of Physics in the Graduate School of Arts and Sciencies of Duke University

1964

ABSTRACT

PROTON-GAMMA ANGULAR CORRELATIONS IN THE $C^{12}(d,p)C^{13}$ REACTION AT LOW ENERGIES

by

Thomas Sidney Katman

Department of Physics
Duke University

Date: _____

Approved:

_____
Robert M. Williamson, Supervisor

_____

_____

_____

_____

An abstract of a dissertation submitted in partial fulfillment of the requirements for the degree of Doctor of Philosophy in the Department of Physics in the Graduate School of Arts and Sciences of Duke University

1964

ABSTRACT

PROTON-GAMMA ANGULAR CORRELATIONS IN THE $C^{12}(d,p)C^{13}$ REACTION AT LOW ENERGIES

by

Thomas Sidney Katman

A study of the $C^{12}(d,p)C^{13}$ reaction leading to the 3.68 and 3.85 MeV states of C^{13} has been made for deuteron energies between 2.0 and 3.0 MeV. Yield curves were obtained at several proton angles, and proton angular distributions were measured for a number of deuteron energies both on and off resonances. Angular correlations between the protons leading to the 3.68 MeV state of C^{13} and the 3.68 MeV γ rays were measured at deuteron energies of 2.35 and 2.50 MeV, both in the reaction plane and in the azimuthal plane perpendicular to the reaction plane symmetry axis. At both energies, the reaction plane correlations retained the full anisotropy observed at higher energies. The correlations were symmetric about the C^{13} recoil axis and the azimuthal anisotropies were approximately zero within the experimental errors. The angular correlations between the protons leading to the 3.85 MeV state of C^{13} and the 3.85 MeV γ rays were measured at deuteron energies of 2.35, 2.50, and 2.6 MeV. Correlations were obtained in the reaction plane and in 2 mutally perpendicular azimuthal planes at each energy.

The data shows that good stripping patterns can exist at low deuteron bombarding energies if the Q value is negative. This phenomenon is evident in both the angular distributions and angular correlations. The very strong 2.50 MeV resonance does not appear to affect the $C^{12}(d,p_3)C^{13}$ angular correlation. Reduced widths have been extracted from the data.

ACKNOWLEDGEMENTS

I would like to thank Dr. R. M. Williamson who suggested this experiment and who guided my graduate studies. I also would like to extend my appreciation to Dr. D. R. Tilley who gave me invaluable assistance throughout measurements and analysis of this experiment. I wish to thank Dr. R. E. Clark for our discussions concerning the mathematical techniques used in the analysis of the data. The assistance of D. G. Gerke, J. Lacambra, J. Sawers, and the entire Van de Graaff group is appreciated. I wish to express thanks to my wife, Roberta, who has typed and corrected this manuscript throughout its history.

This work was supported in part by the United States Atomic Energy Commission.

Thomas Sidney Katman

CONTENTS

LIST OF FIGURES

LIST OF TABLES

PROTON-GAMMA ANGULAR CORRELATIONS IN THE $C^{12}(d,p)C^{13}$ REACTION AT LOW ENERGIES

CHAPTER I

INTRODUCTION

While the plane wave Born approximation analysis of differential cross sections and particle-gamma angular correlation measurements for deuteron stripping reactions[1-4] have provided a great deal of nuclear spectroscopic information such as spins, parities, and reduced widths; the reliability of the information is weakened in many cases by the effects of distortions and compound nucleus contributions. In particular, the interpretation of particle-gamma ray angular correlation patterns, which according to the plane wave Born approximation should constitute straight-forward indicators of the spins and multipolarities, is obscured.[5-11]

The thesis of D. G. Gerke describes an investigation performed to determine whether a detailed distorted wave Born approximation (DWBA) analysis[8,12] of the $C^{12}(d,p)C^{13}$ reaction would give quantitative agreement with the proton angular distribution and proton-gamma angular correlations measured at deuteron energies of 2.8, 3.2 and 3.7 MeV. The quality of the agreement could suggest whether such calculations applied in similar cases

would be of sufficient value in improving the accuracy of the derived spectroscopic information to justify the effort involved.

An alternative approach to the problem follows from the suggestion of Wilkinson[13] that the plane wave description might be very nearly correct for those stripping reactions for which the Q values are negative and the bombarding energies are low. According to this picture, for negative Q and low deuteron energies the proton in a (d,p) reaction needs little momentum; and it can receive this from the deuteron wave function even when the proton-neutron separation is large. Thus, the proton can be far away from the nuclear surface when the neutron is stripped. The optimum energy should be $E_d = -2Q$.[13,14] This suggestion was supported by the measurements of Sellschop and others[15-17] who found that negative Q angular distributions could be matched by the plane wave Born approximation theory. Prompted by this suggestion, Gibbs and Tobocman[18] did some DWBA calculations to test this hypothesis. They found that under these conditions the calculated distortions were not necessarily small but that they could cancel in some cases. A more detailed discussion of endothermic stripping is given in Appendix A.

Since the $C^{12}(d,p)C^{13}$ reactions leaving C^{13} in its second and third excited states have negative Q values, since the spins of the states are known,[19] and since Fletcher, et al[20,21] had studied these reactions at higher energy, it was decided to extend these angular distributions and angular correlation measurements down to an energy which would approximate the optimum conditions suggested by Wilkinson. The energy level diagram of the $C^{12}(d,p)C^{13}$ reactions is shown in Figure 1. Angular correlation investigations under these conditions are scant. Chase, et al[22]

Figure 1. Energy-Level Diagram

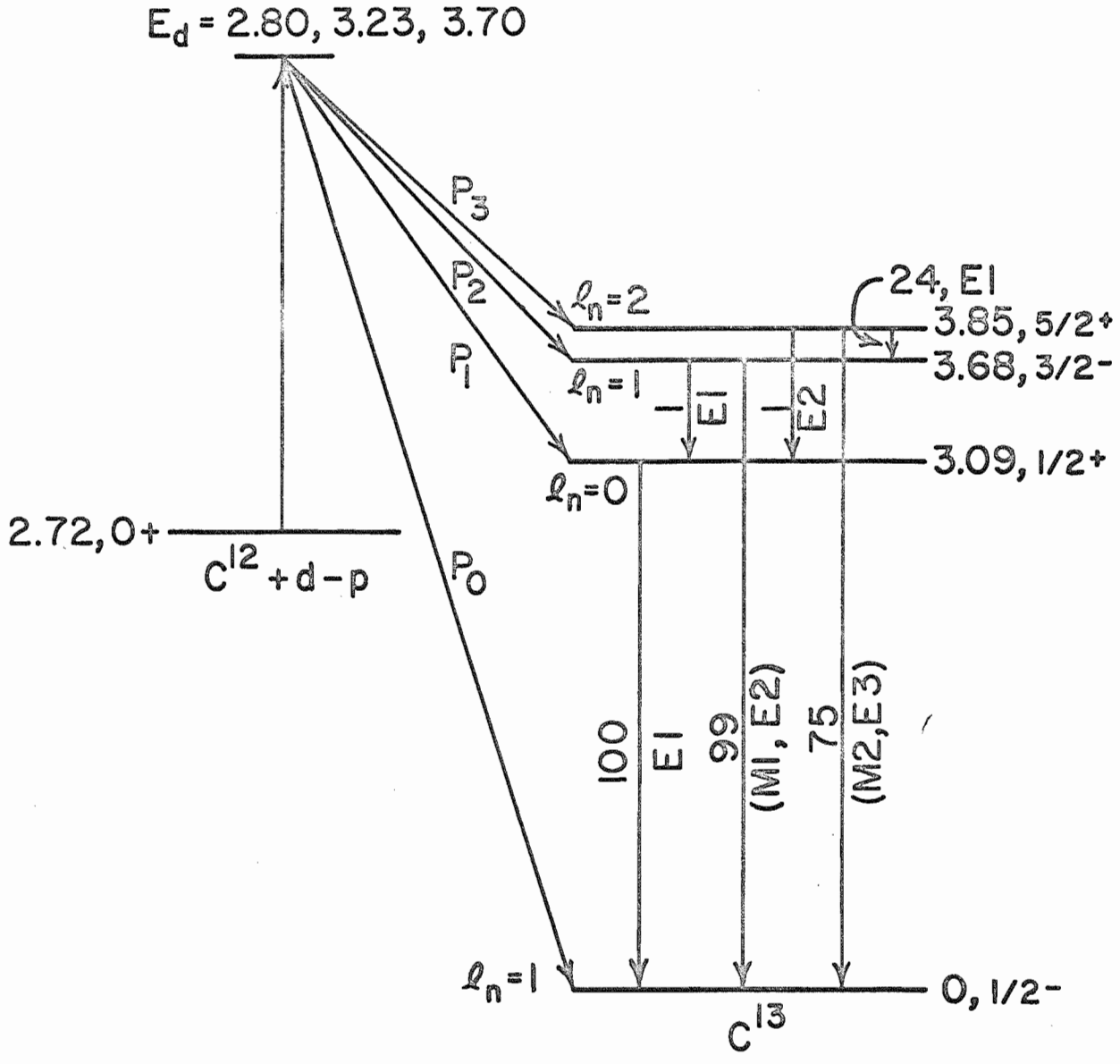

REACTION ENERGY-LEVEL DIAGRAM

measured the angular distribution of the de-excitation gamma rays from the third excited state in C^{13} which is similiar to an angular correlation. It would be particularly useful if negative Q stripping reaction angular correlations measured at low energies could be analyzed reliably by the plane wave theory since the low energy measurements have the experimental advantages of better proton energy resolution and lower gamma ray background.

Since the C^{12} + d yield curves[22-27] in this region are characterized by several prominent resonances, it was also decided to investigate the effect of these resonances upon the stripping angular distributions and angular correlations.

For these purposes, excitation functions of the $C^{12}(d,d)C^{12}$, $C^{12}(d,p_1)C^{13}$, $C^{12}(d,p_2)C^{13}$, and $C^{12}(d,p_3)C^{13}$ reactions were measured at 30°, 47°, 65°, 80.5°, 117°, 134°, and 147° between 2.0 MeV and 3.2 MeV. From these data, seven energies (2.10 MeV, 2.20 MeV, 2.35 MeV, 2.50 MeV, 2.62 MeV, 2.71 MeV, and 2.89 MeV) were chosen at which angular distributions were measured. The energies were chosen so as to approximate the condition $E_d = -2Q$ and so that the energies would be on and off several resonances.

Proton-gamma angular correlations were measured for the reactions leaving C^{13} in the second and third excited state. They were measured near the peaks of the stripping angular distributions at bombarding energies of 2.35 MeV, 2.50 MeV, and 2.62 MeV.

CHAPTER II

EXPERIMENTAL APPARATUS AND PROCEDURE

A. YIELD CURVES AND ANGULAR DISTRIBUTIONS

The target chamber used in measuring the yield curves and the angular distributions is shown in Figure 2. The beam was collimated to within $\pm 0.25^{o}$. Surface barrier detectors having a resolution of 40 keV were used to detect the various reaction products. The counter subtended a solid angle of 2×10^{-4} steradians and an angle of $\pm 1/2^{o}$. In order to reduce carbon buildup on the targets, a liquid air trap was placed near the target. The beam current was measured by a current integrator[28] connected to a Faraday cup placed behind the target. In both sets of measurements the data were normalized to the total charge collected. In order to reduce the effect of secondary electrons, a repeller ring was placed between the target and the Faraday cup.

Figure 2. Cross Section Drawing of Scattering Chamber

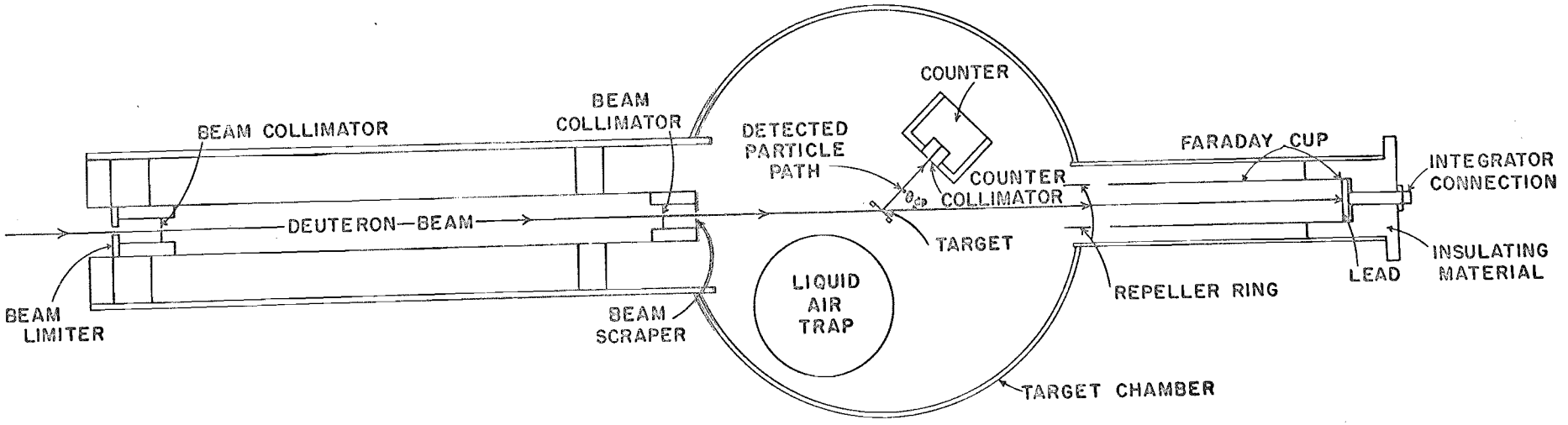
BEAM COLLIMATOR
BEAM COLLIMATOR
COUNTER
DETECTED PARTICLE PATH
FARADAY CUP
INTEGRATOR CONNECTION
COUNTER COLLIMATOR
DEUTERON—BEAM
TARGET
INSULATING MATERIAL
LIQUID AIR TRAP
REPELLER RING
LEAD
BEAM LIMITER
BEAM SCRAPER
TARGET CHAMBER

The deuterons were produced by the Duke University Van de Graaf Accelerator. The deuteron beam bombarded thin self-supporting natural carbon foils.[29] By noting the energy shift of the Li(p,n) threshold[30] when a carbon foil was placed in the beam, the target thickness was determined to be 5 to 10 keV for the deuterons of the energy used in this experiment. The smallest angles at which measurements could be taken were limited by target impurities, the presence of HH^+ in the beam, and the large Rutherford cross section at forward angles. These angles ranged from 20° to 30°. The deuterons used for the yield curve measurements were deflected 60° by the beam steering magnet while the molecular deuteron beam, which was the energy monitor, was deflected 45° by the magnet and then passed through the Duke University 90° electrostatic cylindrical analyser.[31] The cylindrical analyser had been calibrated relative to the Li(p,n) threshold.[30] The energies of the deuterons used while measuring the angular distributions and the angular correlations were determined with a nuclear magnetic resonance magnetometer calibrated by means of the Li(p,n) threshold.[30] The energy of the deuterons could be determined to within 10 keV. A typical pulse height spectrum of the C^{12}+d reaction products is presented in Figure 3.

B. ANGULAR CORRELATIONS

The proton-gamma angular correlations were measured by using the equipment and apparatus described by Fletcher.[20,21] Measurements in the reaction plane (defined by $\vec{k}_d$ and $\vec{k}_r$) and measurements in a plane perpendicular to the reaction plane were made. The angular correlation geometry is shown in Figure 4. The

Figure 3. C^{12} + d Pulse-Height Spectrum

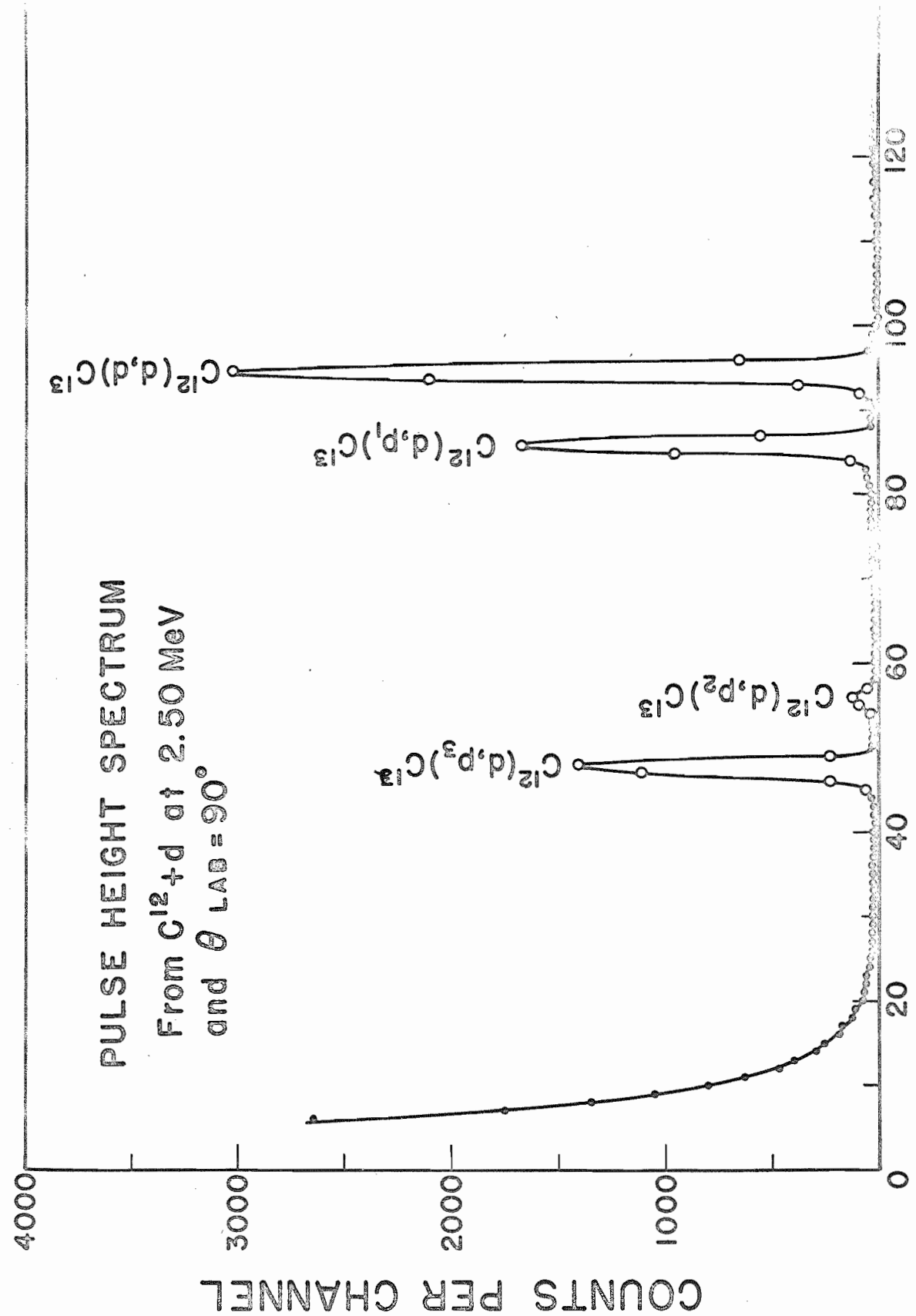
PULSE HEIGHT SPECTRUM
From C^{12}+d at 2.50 MeV
and $\theta_{LAB} = 90°$
$C^{12}(d,p_3)C^{13}$
$C^{12}(d,p_2)C^{13}$
$C^{12}(d,p_1)C^{13}$
$C^{12}(d,d)C^{13}$
COUNTS PER CHANNEL
CHANNEL NUMBER
0
1000
2000
3000
4000
20
40
60
80
100
120

Figure 4. Angular Correlation Geometry

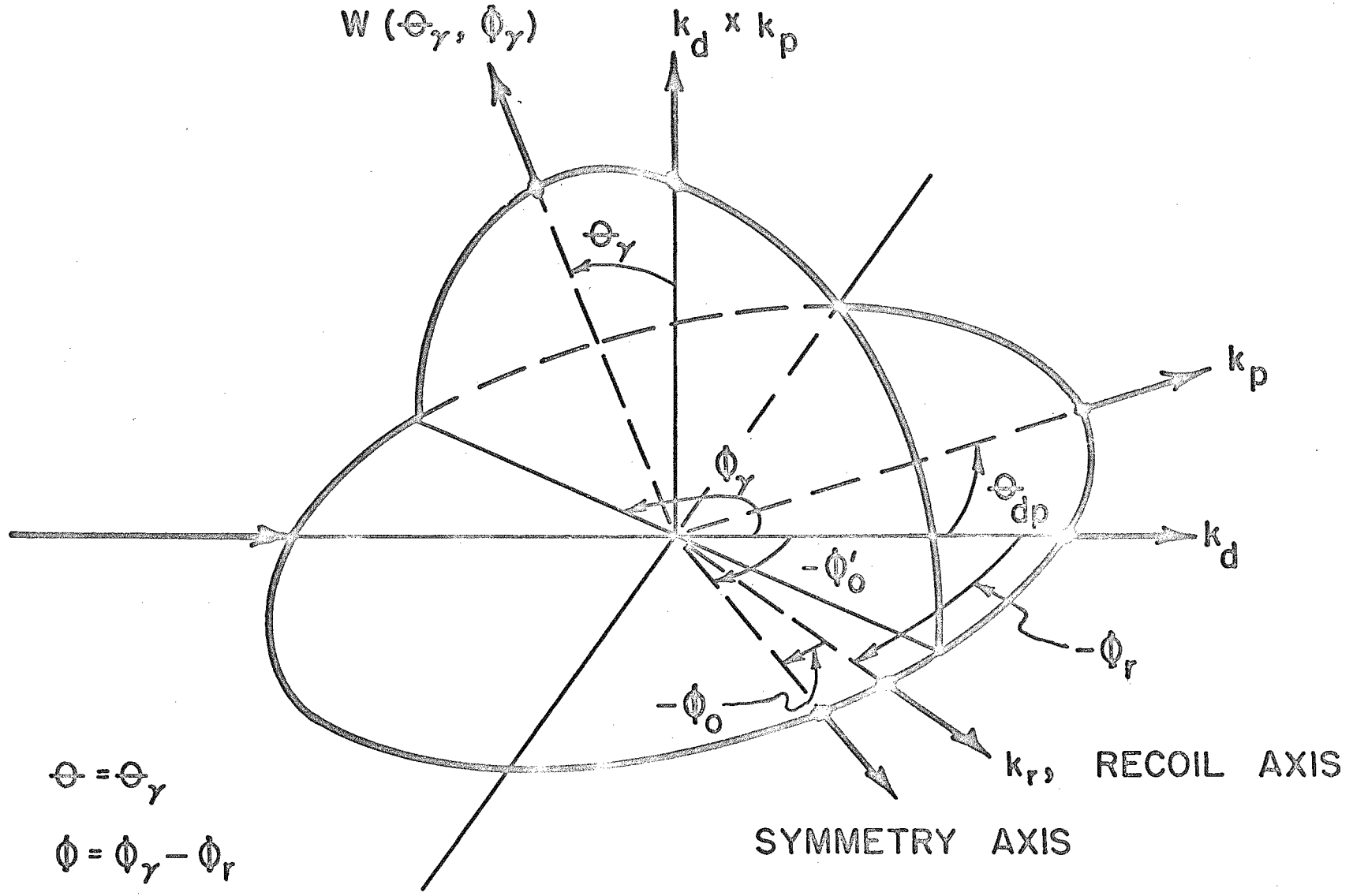
W (Θγ, φγ)
kd x kp
Θγ
kp
φγ
Θdp
kd
-φ'o
-φr
-φo
kr, RECOIL AXIS
SYMMETRY AXIS
Θ = Θγ
φ = φγ − φr

protons were magnetically selected by a momentum spectrometer[32] prior to detection. The geometry of the apparatus was checked by measuring the $C^{12}(d,p_0\gamma)C^{13}$ angular correlation which is isotropic. The $C^{12}(d,p_1\gamma)C^{13}$ angular correlation measurements which were utilized as a check on the geometry of the apparatus are shown in Figure 5.

Figure 5. P_1-γ Angular Correlation at $\theta_{dp} = 20^{o}$ and $E_d = 2.35$ MeV

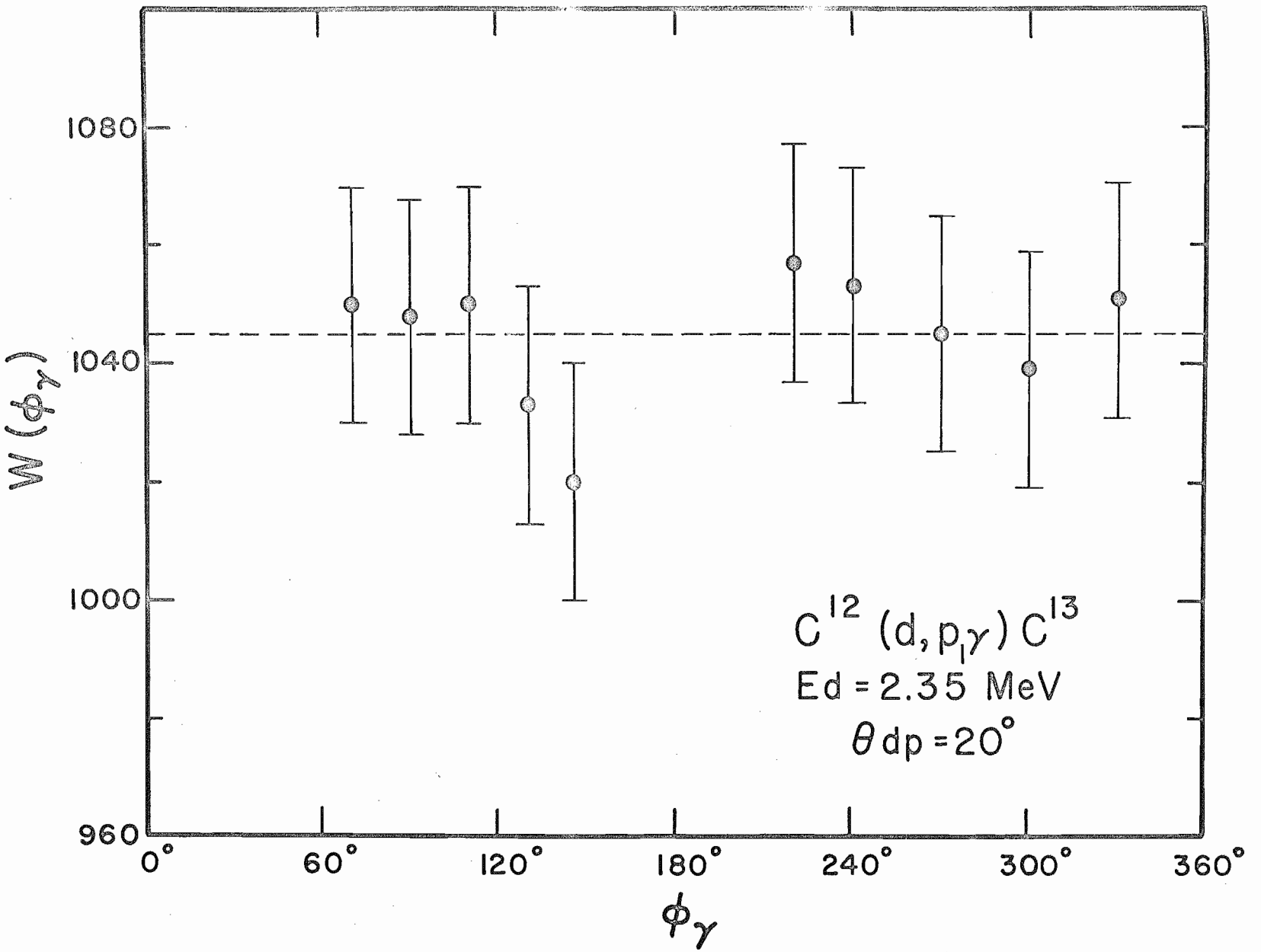
1080
1040
1000
960
W (φγ)
0°
60°
120°
180°
240°
300°
360°
φγ
C12 (d, p1γ) C13
Ed = 2.35 MeV
θ dp = 20°

CHAPTER III

RESULTS

A. YIELD CURVES

Excitation functions of the elastically scattered deuterons and the first three excited state proton groups from the C^{12}+d reactions are shown in Figures 6 to 9. The absolute cross section scale was obtained by normalizing the (d,p_1) data to that of McEllistrem, et al.[23] The normilization was checked at several energies and angles and found to be accurate. The relative errors of the data are due to statistics and background subtraction errors. They do not include a possible $\pm$20% error in the normalization of the data. The relative errors for the $C^{12}(d,d)$, $C^{12}(d,p_1)$ and $C^{12}(d,p_3)$ reactions are approximately $\pm$1%, $\pm$3%, and $\pm$2% to7% respectively. The resonances previously reported [19,23] can be seen in the various yield curves. The agreement of the data of this experiment and that of the other authors is good. The laboratory angles at which the yield curves were measured

Figure 6. $C^{12}(d,d)C^{12}$ Yield Curves

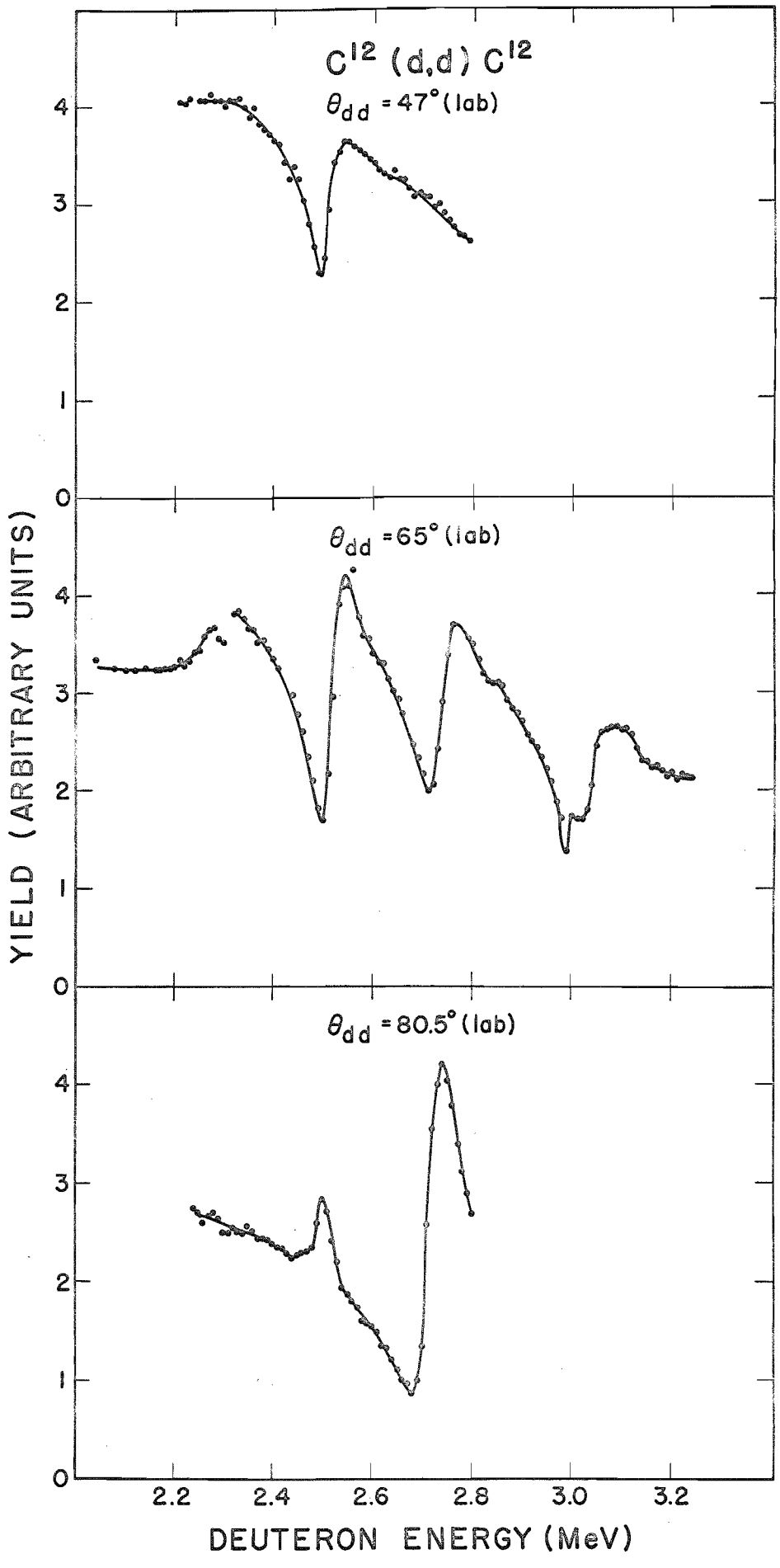
C12 (d,d) C12
θdd = 47° (lab)
θdd = 65° (lab)
θdd = 80.5° (lab)
YIELD (ARBITRARY UNITS)
DEUTERON ENERGY (MeV)
0
1
2
3
4
2.2
2.4
2.6
2.8
3.0
3.2

Figure 7. $C^{12}(d,p_1)C^{13}$ Yield Curves

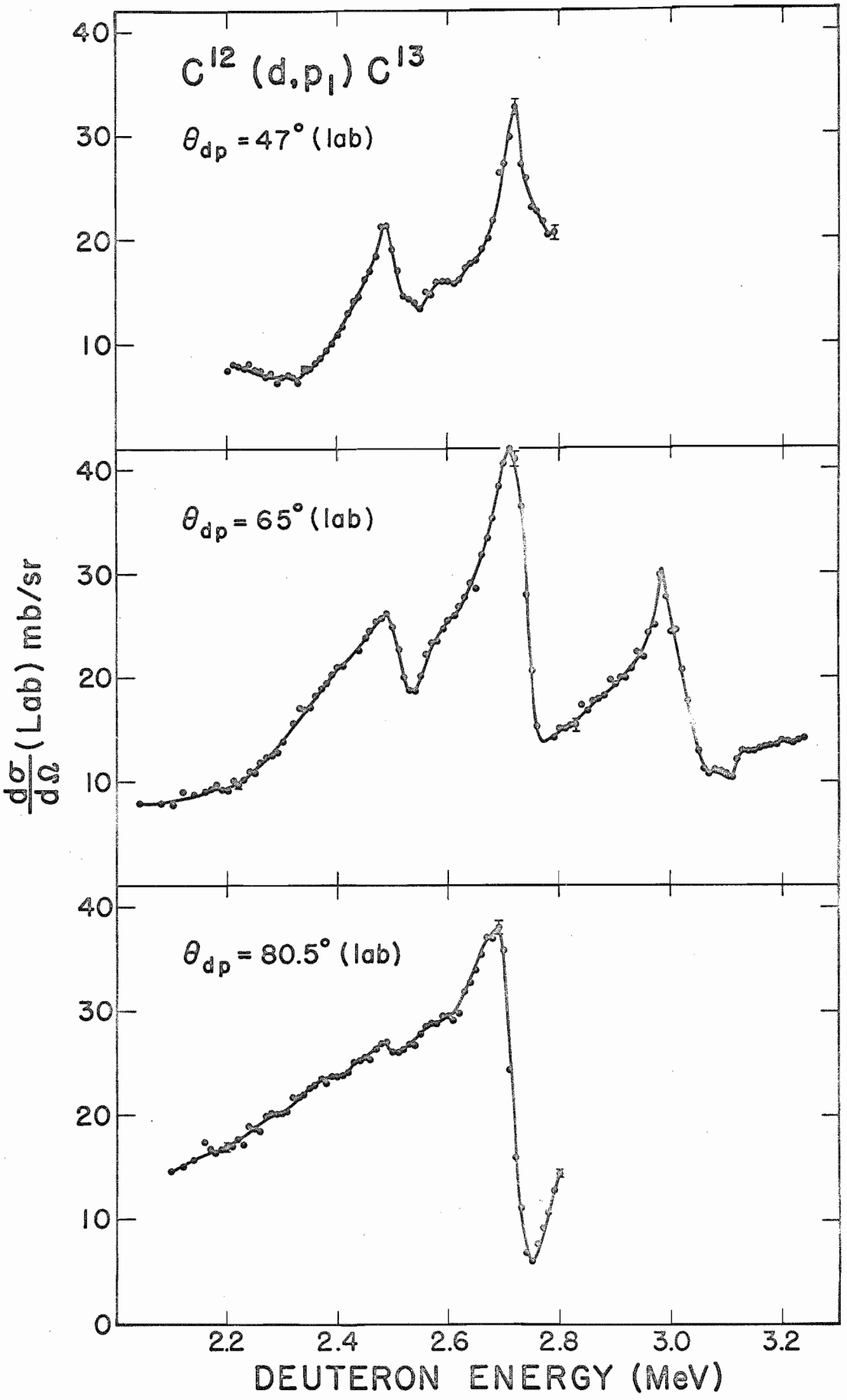
$C^{12}(d,p_1)C^{13}$
$\theta_{dp} = 47°$ (lab)
$\theta_{dp} = 65°$ (lab)
$\theta_{dp} = 80.5°$ (lab)
$\frac{d\sigma}{d\Omega}$ (Lab) mb/sr
0
10
20
30
40
2.2
2.4
2.6
2.8
3.0
3.2
DEUTERON ENERGY (MeV)

Figure 8. $C^{12}(d,p_2)C^{13}$ Yield Curves

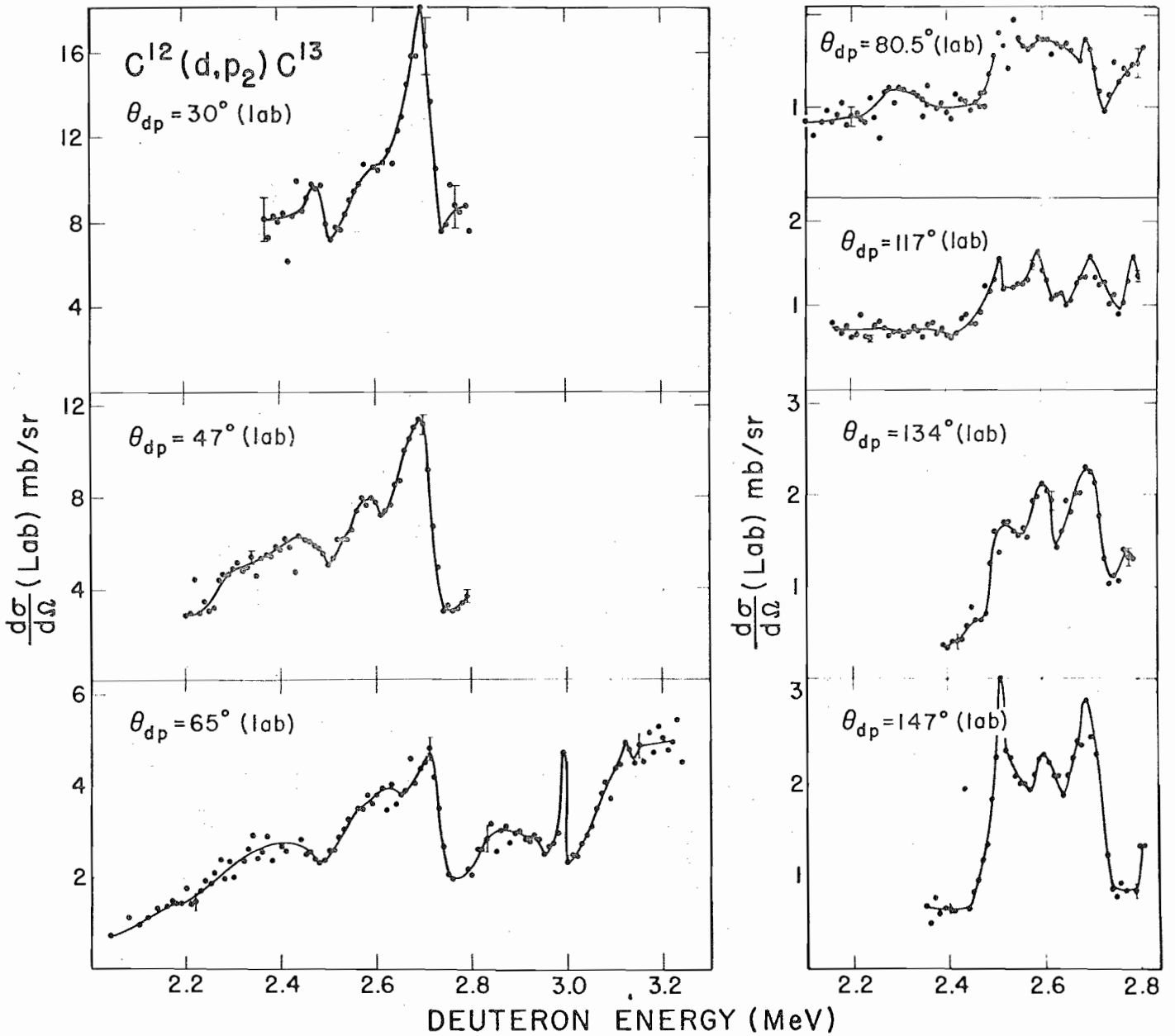
$C^{12}(d,p_2)C^{13}$
θ_{dp} = 30° (lab)
θ_{dp} = 47° (lab)
θ_{dp} = 65° (lab)
θ_{dp} = 80.5° (lab)
θ_{dp} = 117° (lab)
θ_{dp} = 134° (lab)
θ_{dp} = 147° (lab)
$\frac{d\sigma}{d\Omega}$ (Lab) mb/sr
DEUTERON ENERGY (MeV)

Figure 9. $C^{12}(d, p_3)C^{13}$ Yield Curves

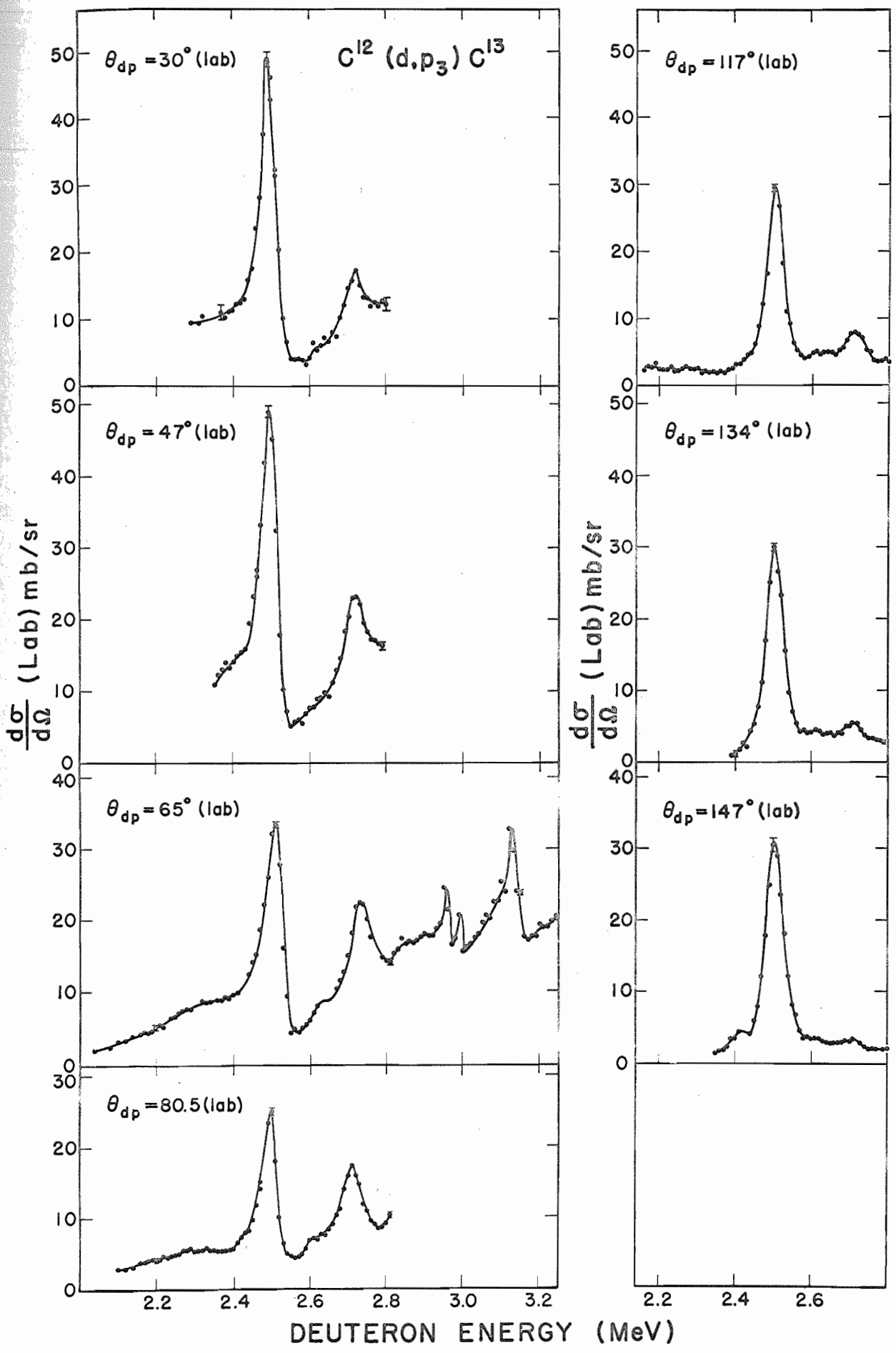
$C^{12}(d,p_3)C^{13}$
θ_{dp} = 30° (lab)
θ_{dp} = 47° (lab)
θ_{dp} = 65° (lab)
θ_{dp} = 80.5 (lab)
θ_{dp} = 117° (lab)
θ_{dp} = 134° (lab)
θ_{dp} = 147° (lab)
$\frac{d\sigma}{d\Omega}$ (Lab) mb/sr
DEUTERON ENERGY (MeV)

were picked so that the angles in the center of mass system were near zeroes of Legendre polynomials in order to aid in possible analysis at a later date. The main reason for the various yield curves was to determine the energies at which interesting angular distributions and angular correlations could be measured. No detailed discussion of the levels in N^{14} will be made.

In the p_1 yield curve the 2.50 MeV and 2.71 MeV resonances show up prominently at the forward angles, while the 2.50 MeV resonance vanishes at 80.5°. For the p_2 yields the 2.50 MeV and 2.62 MeV resonances are relatively more pronounced at the backward angles which could be indicative of compound nuclear formation in addition to stripping while the resonance at 2.71 MeV is clearly seen at all angles in all of the p_2 yield curves. The 2.50 MeV resonance is strong while the 2.62 MeV resonance appears only weakly in the p_3 yields. For the p_3 yields the 2.71 MeV resonance is relatively weaker at the backward angles, contrary to what is normally expected when the stripping mechanism and the compound nuclear formation mechanism are competing.

B. ANGULAR DISTRIBUTIONS

The angular distributions of the p_1, p_2, and p_3 groups are shown in Figures 10 to 12 along with the Butler-Born approximation fits as calculated using a form equivalent to equation 34 of reference 3. These groups have been measured previously[23,24,26,33,34] and are known to correspond to ln = 0, ln = 1, and ln = 2 respectively. The deuteron energies were selected to bracket the strong C^{12}+d resonances and in addition were extended to as low an energy as was experimentally feasible. The relative error

Figure 10. $C^{12}(d,p_1)C^{13}$ Angular Distributions

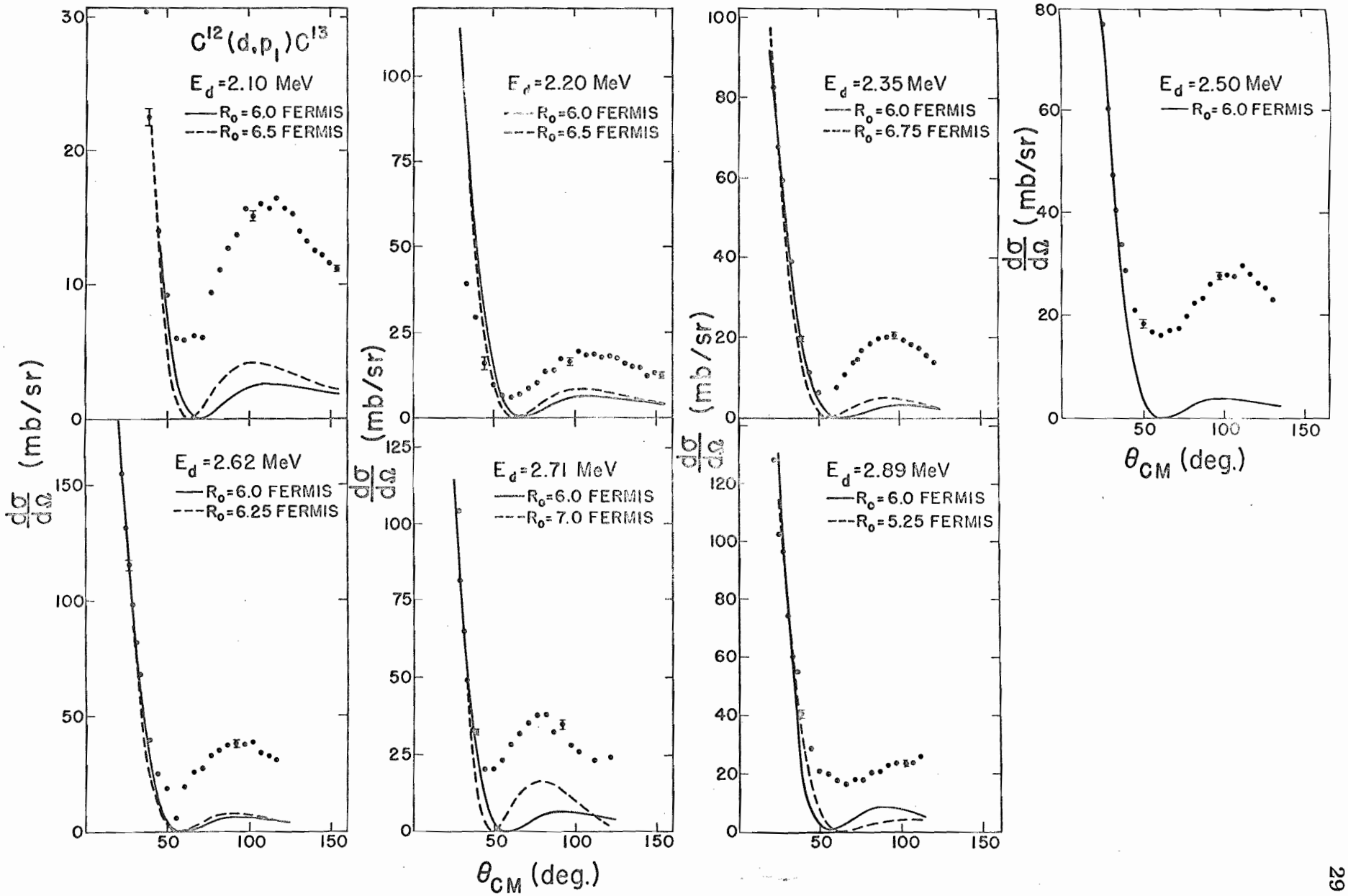
$C^{12}(d,p_1)C^{13}$
E_d = 2.10 MeV
R_0 = 6.0 FERMIS
R_0 = 6.5 FERMIS
E_d = 2.20 MeV
R_0 = 6.0 FERMIS
R_0 = 6.5 FERMIS
E_d = 2.35 MeV
R_0 = 6.0 FERMIS
R_0 = 6.75 FERMIS
E_d = 2.50 MeV
R_0 = 6.0 FERMIS
E_d = 2.62 MeV
R_0 = 6.0 FERMIS
R_0 = 6.25 FERMIS
E_d = 2.71 MeV
R_0 = 6.0 FERMIS
R_0 = 7.0 FERMIS
E_d = 2.89 MeV
R_0 = 6.0 FERMIS
R_0 = 5.25 FERMIS
$\frac{d\sigma}{d\Omega}$ (mb/sr)
θ_{CM} (deg.)

Figure 11. $C^{12}(d,p_2)C^{13}$ Angular Distributions

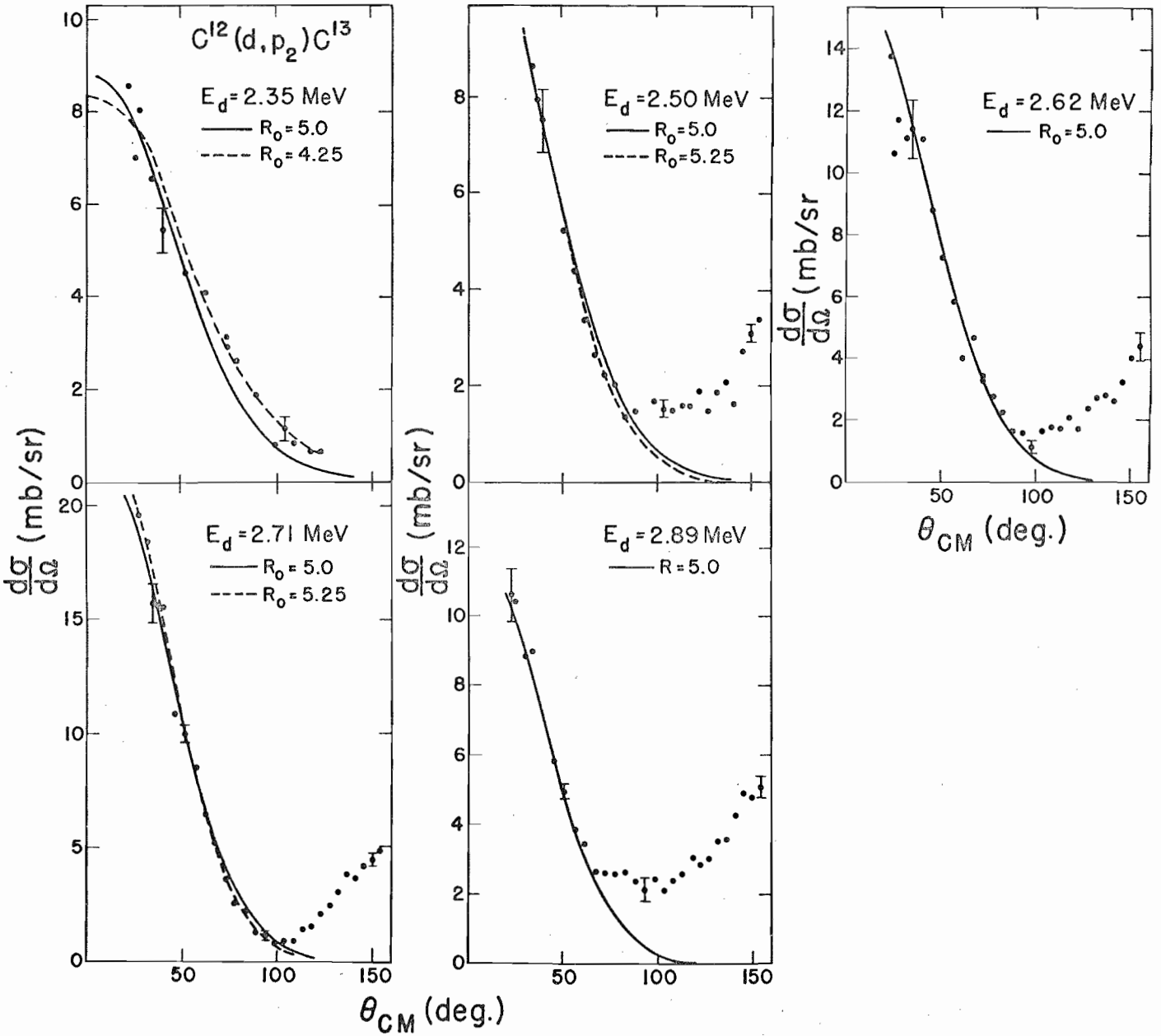
$C^{12}(d,p_2)C^{13}$
E_d = 2.35 MeV
R_0 = 5.0
R_0 = 4.25
E_d = 2.50 MeV
R_0 = 5.0
R_0 = 5.25
E_d = 2.62 MeV
R_0 = 5.0
E_d = 2.71 MeV
R_0 = 5.0
R_0 = 5.25
E_d = 2.89 MeV
R = 5.0
$\frac{d\sigma}{d\Omega}$ (mb/sr)
θ_{CM} (deg.)

Figure 12. $C^{12}(d,p_3)C^{13}$ Angular Distributions

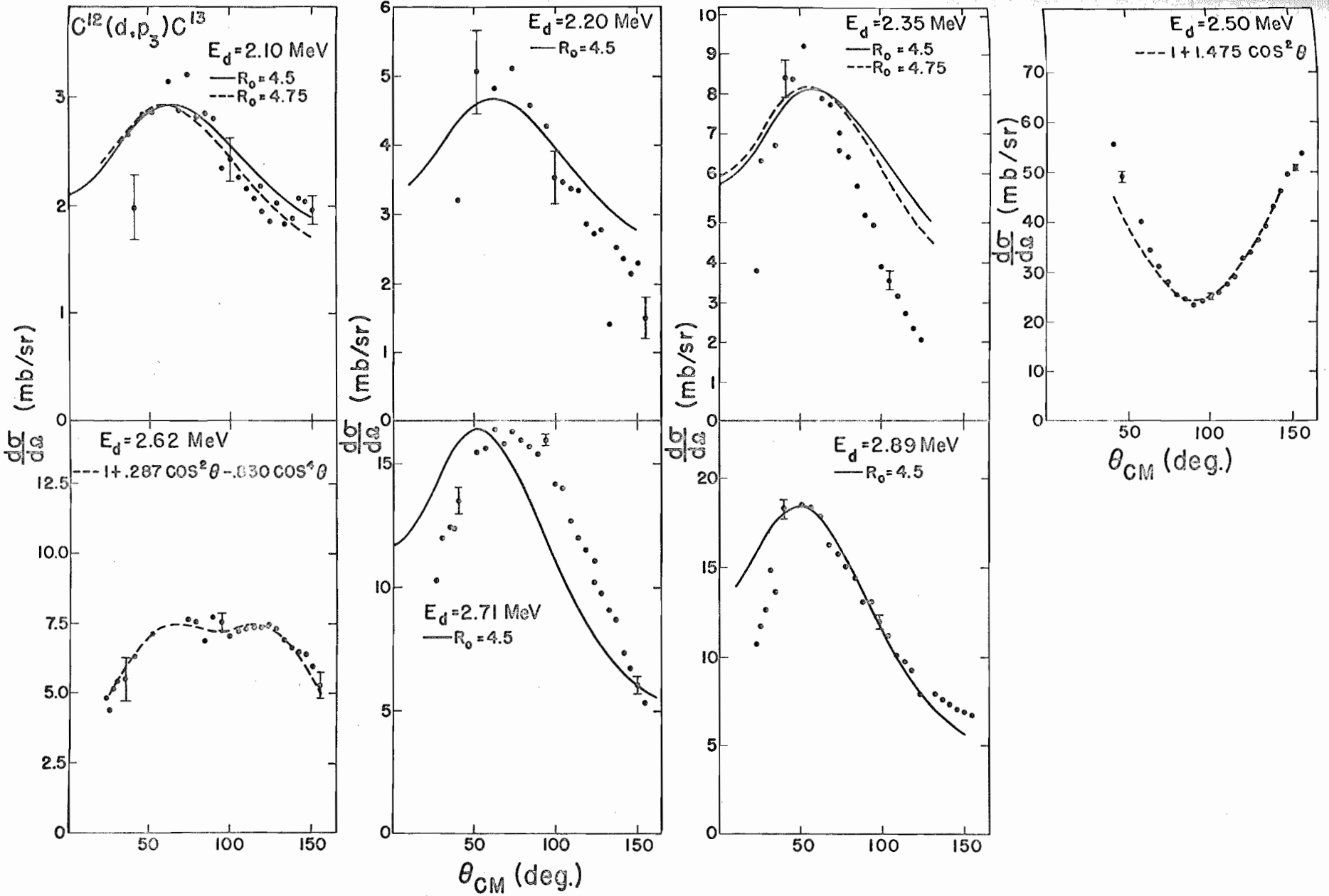
$C^{12}(d,p_3)C^{13}$
E_d = 2.10 MeV
R_0 = 4.5
R_0 = 4.75
E_d = 2.20 MeV
R_0 = 4.5
E_d = 2.35 MeV
R_0 = 4.5
R_0 = 4.75
E_d = 2.50 MeV
$1+1.475\cos^2\theta$
E_d = 2.62 MeV
$1+.287\cos^2\theta-.030\cos^4\theta$
E_d = 2.71 MeV
R_0 = 4.5
E_d = 2.89 MeV
R_0 = 4.5
$\frac{d\sigma}{d\Omega}$ (mb/sr)
θ_{CM} (deg.)

bars shown do not include a possible $\pm 20\%$ error in the normalization of the data.

The p_1 angular distributions at forward angles are well matched by the calculated fits, although the experimental points at backward angles are larger than that predicted by theory. The shapes of the p_1 angular distributions appear to be rather independent of energy even when measured on a resonance. The positions of the first minima and the second maxima of the p_1 angular distributions are in general agreement with the observations of Hamburger,[33] which were that they occur at larger angles as the energy of the deuterons is lowered.

The measured p_2 angular distribution and the calculated angular distribution at 2.35 MeV are in good agreement. Above 2.35 MeV the cross sections show a back angle peaking which suggests compound nuclear formation but this effect can also be caused by distortions. It is interesting that the angular distribution, which was measured at the lowest deuteron energy and hence, most near the condition specified by Wilkinson, was well matched by the plane wave theory.

The measured p_3 angular distributions at 2.10 MeV, 2.20 MeV, 2.35 MeV, 2.71 MeV, and 2.89 MeV are more narrow than the Butler curves as were those of D. G. Gerke[26] and contrary to the majority of (d,p) measurements. The angular distributions at 2.50 MeV and 2.62 MeV are nearly symmetric about 90°, which is a characteristic of compound nucleus formation. Least square fits of the form $\sum_{n=0}^{K} A_{2n} P_{2n}(\cos\theta)$ are shown along with the p_3 data at 2.50 MeV and 2.62 MeV. The value of K in these two cases was determined by the use of Gauss' criterion for the best fit.

Using the method suggested by Macfarlane and French,[35] reduced widths have been extracted from the p_1, p_2, and p_3 angular distributions of this experiment and those of Gerke, et al. These reduced widths are listed in Table I along with those tabulated by Macfarlane and French[35] for the p_0, p_1, p_2, p_3 angular distributions. A discussion of reduced widths and the procedure used for extracting them is given in Appendix B.

The larger p_1 reduced widths at 2.62 MeV and 2.71 MeV might be explained by the increased cross section due to resonances. The fact that the 2.50 MeV resonance does not appear to have an effect on the p_1 reduced width is interesting. The value of the low energy p_2 reduced widths appear to follow the cross section magnitude. In the p_3 case an interesting feature is that the reduced widths have nearly a linear increase with energy from 2.10 MeV to 3.70 MeV. It must be noted, however, that the strong resonance region of 2.50 MeV to 2.71 MeV was omitted from the tabulation. This omission was due to the compound nucleus appearance of the angular distributions.

The $C^{12}(d,p_0)C^{13}$ reduced widths increase by about a factor of 2 when the energy is increased from 2.68 MeV to 8 MeV. The $C^{12}(d,p_1)C^{13}$ and the $C^{12}(d,p_3)C^{13}$ reduced widths increase by several factors of 2 when the deuteron bombarding energy is increased from a few MeV up to a value of 8 or 9 MeV. This is in agreement with the reduced width energy variation in other reactions. See page 682 of reference 35. The $C^{12}(d,p_2)C^{13}$ reduced widths below 3.70 MeV are not consistently smaller than those reduced widths extracted at high energy.

TABLE I

ABSOLUTE VALUES
OF

THE REDUCED WIDTH FROM
STRIPPING ANALYSIS OF $C^{12}(dp)C^{13}$

INCIDENT ENERGY (MeV)	$C^{12}(dp_o)C^{13}$	$C^{12}(dp_1)C^{13}$	$C^{12}(dp_2)C^{13}$	$C^{12}(dp_3)C^{13}$
2.10	----	.031	----	.004
2.20	----	.036	----	.008
2.35	----	.042	.0029	.011
2.50	----	.039	.0034	----
2.62	----	.068	.0045	----
2.68	.022	----	----	----
2.71	----	.090	.0066	----
2.80	----	----	.0027	.022
2.89	----	.040	.0034	.025
3.20	----	----	.0063	.027
3.29	.025	----	----	----
3.70	----	----	.0056	.046
8.0	.056	.18	.006	.098
9.0	.042	.19	.013	.073
14.8	.031	.15	.006	.071

Macfarlane and French[35] have stated that the reduced widths extracted from data measured below 5 MeV are often subject to rapid variations. This can be seen in the present data.

C. ANGULAR CORRELATIONS

The p_2-gamma reaction plane angular correlations measured at 2.35 MeV and 2.50 MeV are shown in Figure 13. They were measured at a proton angle of 20° relative to the deuteron beam. The spin of the second excited state in C^{13} is 3/2 so only terms through the second order appear in the correlation function. Least square fits of the form $W(\phi_\gamma) = 1+\alpha\cos^2(\phi_\gamma - \phi'_o)$ are shown. α and ϕ'_o were the variable parameters. If the plane wave description is valid, $\phi'_o = \phi_r$ where ϕ_r is the angle of C^{13} recoil axis, while DWBA predicts a possible shift in the symmetry axis away from ϕ_r. The plane wave Born approximation theory predicts that the azimuthal correlation measured in a plane perpendicular to the C^{13} recoil axis should be isotropic while DWBA predicts that an anisotropy of the form $W(\theta) = 1+\beta\cos^2\theta$ can occur. The p_2 gamma angular correlation parameters of this experiment along with those measured by Fletcher[20,21] are listed in Table II. The measured reaction plane correlations have the recoil axis as the axis of symmetry unlike the higher energy data, and in this sense the lower energy data are more compatable with the plane wave picture. The values of β, obtained from the low energy azimuthal correlations are essentially zero as they are in the higher energy data measurements. It will be noted that the reaction plane angular correlation at 2.50 MeV has an anisotropy as large as the largest anisotropy measured at higher

Figure 13. P_2-γ Angular Correlations at $\Theta_{dp} = 20^{o}$ and $E_d = 2.35$ and 2.50 MeV

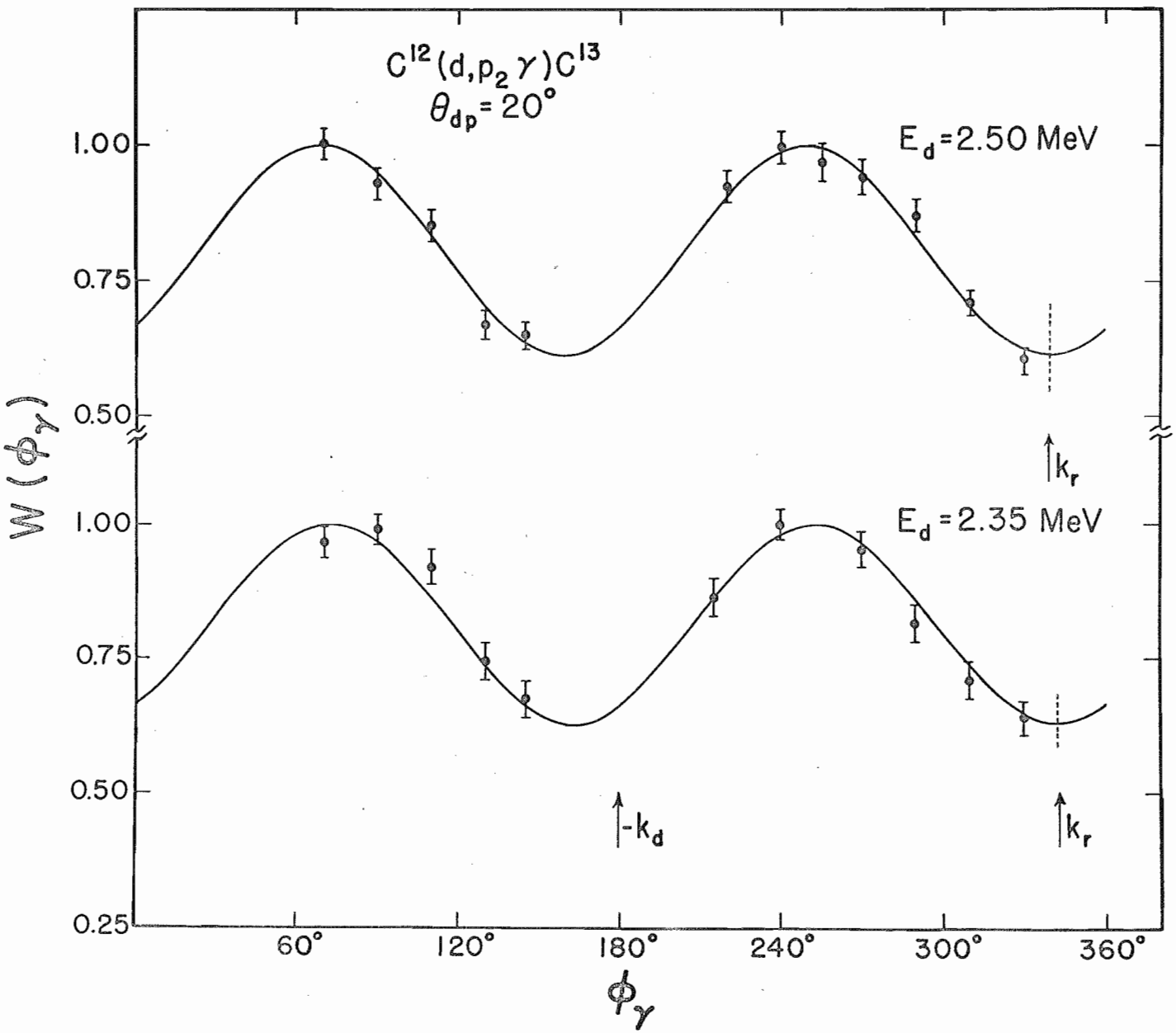
$C^{12}(d,p_2\gamma)C^{13}$
$\theta_{dp}=20°$
$E_d=2.50$ MeV
$E_d=2.35$ MeV
$W(\phi_\gamma)$
1.00
0.75
0.50
0.25
k_r
$-k_d$
60°
120°
180°
240°
300°
360°
ϕ_γ

TABLE II

P_2-γ CORRELATION PARAMETERS

E_d	α [a]	$-\phi_o'$ [b]	$-\phi_r$	β [a]	g_2 [c]	λ [d]
2.35	-0.394±0.032	17°±3°	17°	+0.078±0.062	-0.41±0.10	0.72±0.16
2.50	-0.411±0.022	21°±3°	20°	+0.043±0.054	-0.38±0.08	0.83±0.18
2.80	-0.280±0.050	30°±5°	21°	+0.026±0.023	-0.24±0.05	
3.23	-0.360±0.030	36°±3°	22°	+0.022±0.027	-0.30±0.05	0.89±0.17
3.70	-0.400±0.030	44°±3°	24°			

a) Coefficients have been corrected for finite solid angle.

b) Angular errors include 1° absolute errors. All other errors are statistical.

c) Calculated from $g_2 = (2\alpha - 4\beta)(3 + \beta + \alpha)$.

d) Calculated from $\lambda = \alpha(\alpha - 2\beta)$.

energies even though it was measured on a large C^{12}+d resonance. The resonance has no apparent effect on the shape of the correlation. The mixing ratio of the gamma rays from the 3.68 MeV level in C^{13} is not independently known. However, a value can be determined if the correlation with the largest anisotropy is assumed to be unattenuated. From the 2.50 MeV data the result $\Gamma(E2)/\Gamma(\gamma) = 0.010 \pm^{.0022}_{.0020}$ is obtained. This agrees well with the value of $\Gamma(E2)/\Gamma(\gamma) = .01 \pm .003$ obtained by Fletcher, et al.[20,21]

The DWBA parameters and g_2 are also listed in Table II. For an $\ell n = 1$ nucleon capture $\lambda = \alpha(\alpha - 2\beta)$ and $g_2 = \frac{2(\alpha - 2\beta)}{3+\beta+\alpha}$. λ is the distortion parameter as defined by Huby, et al[4]. λ has a minimum value of 0 and in the plane wave limit a value of 1. This implies that α and β must have opposite signs. If deuteron stripping is the only contributing mechanism, g_2 is supposed to be energy independent. It appears to be constant. However, this may not be very significant because the form of the equation defining g_2 magnifies any errors.

The reaction plane p_3-gamma angular correlations are shown in Figure 14. They were measured at a proton angle of 40° relative to the deuteron beam. The spin of the third excited state in C^{13} is 5/2 so only terms through the fourth order appear in the correlation function. Least square fits of the form $1 + A_2P_2(\cos \phi_\gamma - \phi'_o) + A_4P_4\cos(\phi_\gamma - \phi'_o)$ and $1 + b_2\cos 2(\phi_\gamma - \alpha_{22}) + b_4\cos 4(\phi_\gamma - \alpha_{44})$ are shown along with the data. The first of these two forms is the plane wave prediction except that ϕ'_o has been allowed to be arbitrary. In the plane wave description $\phi'_o = \phi_r$. The second form is that predicted by DWBA. The p_3-gamma angular correlation parameters are listed in Table III

Figure 14. P_3-γ Angular Correlations at $\Theta_{dp} = 40^{o}$ and $E_d = 2.35$, 2.50, and 2.62 MeV

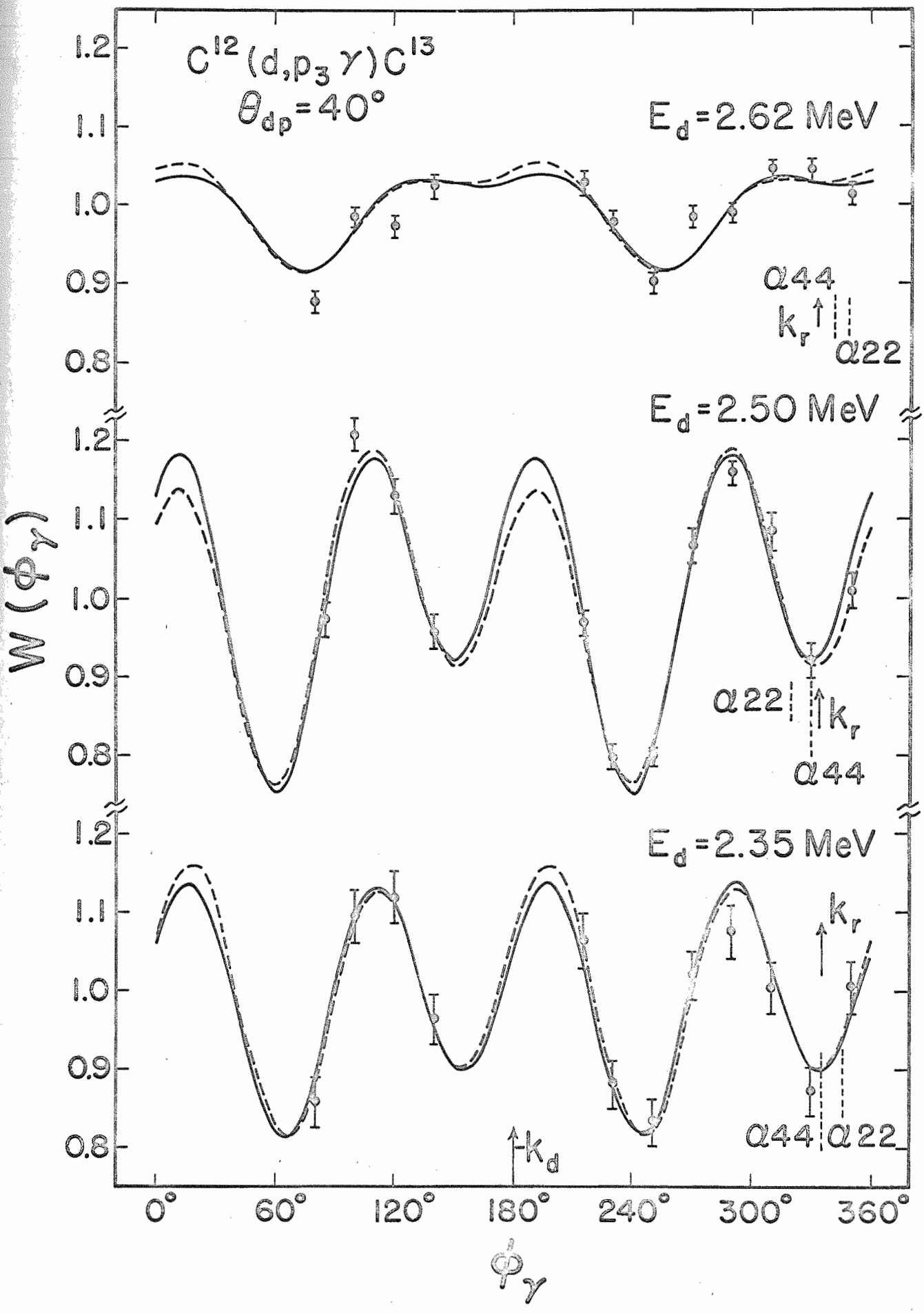
$C^{12}(d,p_3\gamma)C^{13}$
$\theta_{dp}=40°$
$E_d=2.62$ MeV
$E_d=2.50$ MeV
$E_d=2.35$ MeV
$W(\phi_\gamma)$
ϕ_γ
α_{44}
α_{22}
k_r
k_d
1.2
1.1
1.0
0.9
0.8
0°
60°
120°
180°
240°
300°
360°

along with the data of Fletcher.[20,21] The reaction plane angular correlations measured at 2.35 MeV and 2.50 MeV and have the general appearance of the higher energy data, although they are not as anisotropic. It will be noted that ϕ'_o approximates ϕ_r unlike the higher energy data. The azimuthal correlations were measured in a plane perpendicular to $\vec{k}_r$ and also measured in the plane containing $\vec{k}_d \times \vec{k}_r$ and $\vec{k}_r$. If the plane wave theory were correct, the azimuthal correlations would be isotropic while the latter would be identical to the reaction plane correlation. The DWBA theory allows departure from these predictions. The plane wave predictions are shown along with the azimuthal correlation data in Figure 15. The reaction plane correlations and the azimuthal correlations appear to be compatible with the plane wave description. It is interesting to note that the very strong 2.50 MeV resonance does not greatly alter the general shape of the correlations measured at this energy even though the angular distribution was greatly affected.

The angular correlations measured at a deuteron energy of 2.62 MeV have an appearance unlike any of the other p_3 correlations. It will be remembered that this was an energy at which the angular distribution had a form suggestive of compound nucleus formation. Chase, et al[22] noted an anomaly at this energy when measuring the angular distribution of the cascade gamma ray between the third and second excited states in C^{13}. A small resonance appears at this energy in the yield curves in Figure 9 as well as the total yield curves as measured by Chase, et al.[22] It would appear that some mechanism in addition to stripping occurs at this energy for the $C^{12}(d,p_3)C^{13}$ reaction.

TABLE III

P_3-γ CORRELATION PARAMETERS

E_d	A_2/A_o	A_4/A_o	a_2/a_o	a_4/a_o	$-\phi_o'$
2.35	1.89±0.18	-1.82±0.20	0.174±0.02	-0.328±0.04	25.9°±3°
2.50	2.61±0.10	-2.41±0.12	0.261±0.01	-0.397±0.02	30.2°±3°
2.62	0.43±0.11	-0.25±0.11	0.131±0.01	-0.052±0.02	14.6°±3°
2.80	2.68±0.2	-2.60±0.2	0.224±0.02	-0.431±0.04	44.4°±3°
3.23	2.55±0.2	-2.46±0.2	0.223±0.02	-0.412±0.03	47.5°±3°
3.70	2.71±0.2	-2.64±0.2	0.221±0.02	-0.438±0.03	47.3°±3°

	b_2/b_o	b_4/b_o	α_{22}	α_{44}	$-\phi_r$
2.35	0.046±0.017	-0.146±0.018	14°±13°	25°±3°	25°
2.50	0.080±0.008	-0.161±0.009	40°±6°	30°±3°	26°
2.62	0.058±0.015	-0.029±0.013	11°±9°	18°±9°	27°
2.80	0.068±0.014	-0.248±0.02	35°±8°	47°±2°	28°
3.23	0.063±0.014	-0.222±0.02	32°±7°	47°±2°	29°
3.70	0.049±0.013	-0.242±0.02	21°±7°	44°±2°	30°

$$W(\phi_\gamma) = \sum_\nu A_\nu \cos(\phi_\gamma - \phi_o')$$
$$= \sum_\nu a_\nu P_\nu [\cos(\phi_\gamma - \phi_o')]$$
$$= \sum_\nu b_\nu \cos^\nu(\phi_\gamma - \alpha_{\nu\nu})$$

All angular errors include 1° absolute error in ϕ_o.

All coefficients have been corrected for finite detectors.

Figure 15. P_3-γ Azimuthal Correlations at $\theta_{dp} = 40^{o}$ and $E_d = 2.35$, 2.50, and 2.62 MeV

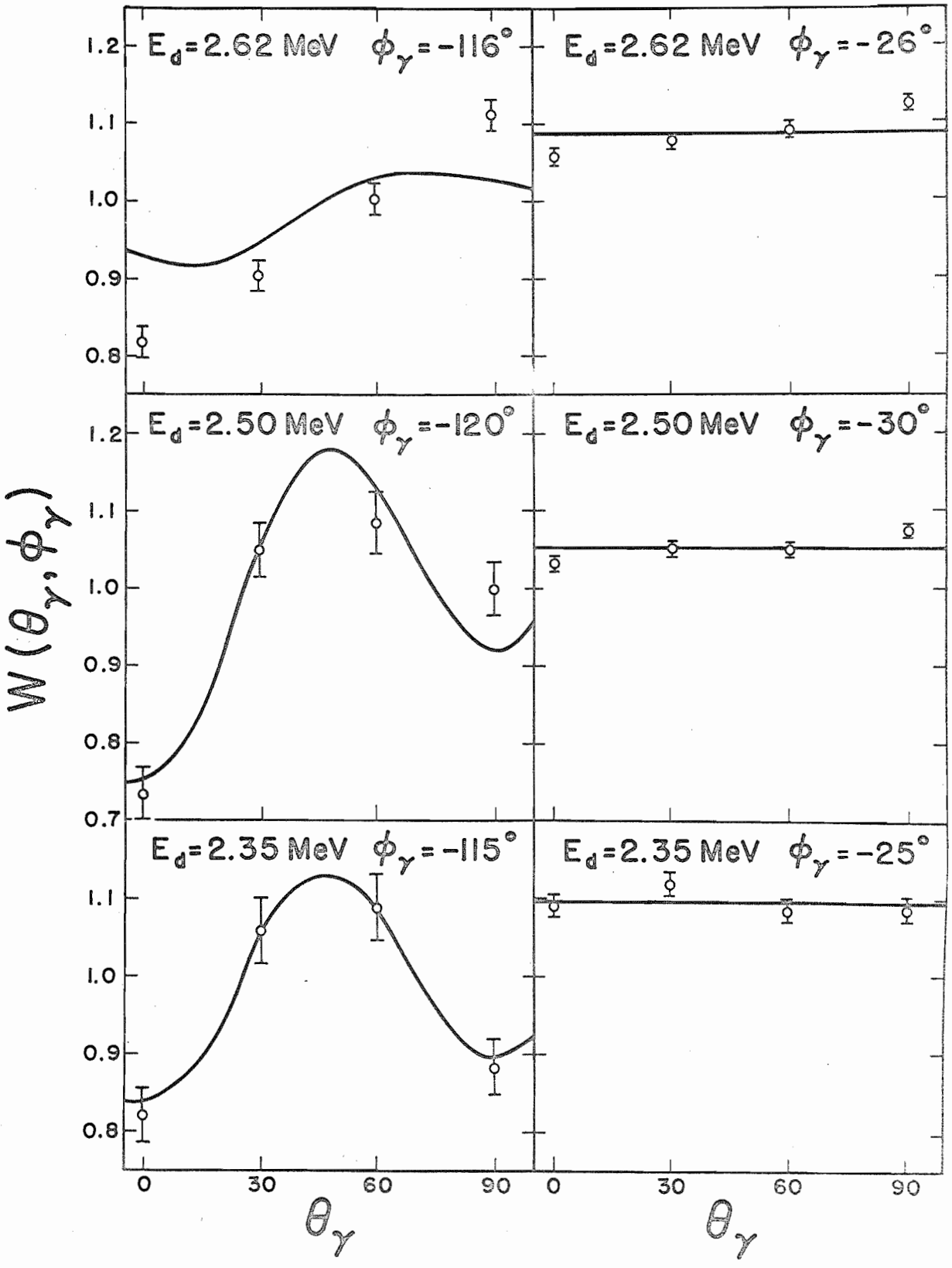
E_d=2.62 MeV ϕ_γ=-116°
E_d=2.62 MeV ϕ_γ=-26°
E_d=2.50 MeV ϕ_γ=-120°
E_d=2.50 MeV ϕ_γ=-30°
E_d=2.35 MeV ϕ_γ=-115°
E_d=2.35 MeV ϕ_γ=-25°
$W(\theta_\gamma, \phi_\gamma)$
θ_γ
θ_γ
0
30
60
90
0.7
0.8
0.9
1.0
1.1
1.2

CHAPTER IV

CONCLUSIONS

A. RESONANCE EFFECTS

In the non-resonant regions most of the angular distributions and angular correlations have definite stripping patterns. The $C^{12}(d,p_1)$ angular distribution has a good stripping pattern at the 2.50 MeV resonance. The $C^{12}(d,p_2)$ reaction has a good stripping pattern in the angular distribution and in the angular correlations at 2.50 MeV. The possible explanation of the good stripping patterns in the p_1 and p_2 groups is that the resonance amplitude is small compared to the non-resonance amplitude at this energy. The $C^{12}(d,p_3)$ angular distribution does not appear to have a stripping shape at 2.50 MeV. This is not surprising because of the extremely large p_3 resonance at this energy. It is of extreme interest that in the presence of this large resonance amplitude the angular correlation has the appearance of pure plane wave stripping. It is hard to explain this phenomenon. However, the level in N^{14} corresponding to this resonance

has a reduced width for deuterons equal to 0.4 times the Wigner limit, and this level is almost a pure single particle state. The third level in C^{13} has the single particle width for neutron capture while the second level in C^{13} involves core excitation. This might explain why the $C^{12}(d,p_3)$ resonance at 2.50 MeV is so large. DWBA can predict symetric angular distributions and this might explain the appearance of the $C^{12}(d,p_3)$ angular distribution. A direct interaction, type of resonance going through the two single particle states might explain the appearance of the angular correlation at this resonant energy.

The very weak resonance at 2.62 MeV does not effect the $C^{12}(d,p_1)$ and $C^{12}(d,p_2)$ angular distributions very much. However, the $C^{12}(d,p_3)$ angular distribution and angular correlation are greatly effected. A compound nucleus type of mechanism might be present. There is no stripping peak in the angular distribution and the angular correlation does not have the appearance of those measured at other energies. The difference in behavior of the $C^{12}(d,p_1)$, $C^{12}(d,p_2)$, and the $C^{12}(d,p_3)$ angular distributions is hard to explain.

There is a forward peaking in the resonance amplitude of the $C^{12}(d,p)$ reactions at 2.71 MeV. The angular distributions are not greatly effected by this resonance. This is a bit surprising in the case of $C^{12}(d,p_2)$, which shows a rather large resonance amplitude.

B. ENDOTHERMIC DEUTERON STRIPPING

Extraction of reduced widths at low energy does not appear to be practical due to the rapid variation of the reduced width

with energy. The $C^{12}(d,p_3)$ reduced widths increase by a factor of about 10 between 2 MeV and 4 MeV and an additional factor of 1.5 to 2 between 4 MeV and 8 or 14 MeV. The other $C^{12}(d,p)$ groups increase by a factor of 2 to 4 between 4 MeV and 8 or 14 MeV. While the Q values of the $C^{12}(d,p_2)$ and $C^{12}(d,p_3)$ reactions are similiar, they do not behave in the same manner. The larger ℓ value of the $C^{12}(d,p_3)$ reaction may be the reason for the increase with energy of this p_3 reduced width. However, there is not enough data to support conclusively this fact. These data support the observation of Macfarlane and French[35] that reduced widths should not be obtained from data below about 5 MeV.

From the angular distributions of this experiment and of others, it can be seen that the lowest energy at which stripping behavior is evident is 2.5 MeV for $C^{12}(d,p_o)$, $\leq$ 2.1 MeV for $C^{12}(d,p_1)$, $\leq$2.35 MeV for $C^{12}(d,p_2)$, and $\leq$ 2.1 MeV for $C^{12}(d,p_3)$. The best stripping patterns of the $C^{12}(d,p_{2,3})$ reactions are at the lowest energies. At energies higher than 2.1 MeV the observed peaks in the $C^{12}(d,p_3)$ reaction are more narrow than are those predicted by the plane wave Born approximation theory. This is quite unusual. This phenomenon persists up to at least 3.8 MeV.[20,21] From the $C^{12}(d,p_o)$ data[23] and the data of Cox and Williamson[11] it can be seen that positive Q stripping patterns at these low energies are poorly matched by plane wave calculations. The low energy negative Q angular distributions of this experiment lend support to the hypothesis that negative Q low energy stripping reactions might be well matched by the plane wave theory.

The symmetry axis of a deuteron stripping angular correlation is the recoil axis in the plane wave picture. The anisotropy of the angular correlation may be calculated and is energy independent according to the plane wave theory. A comparison of the measured symmetry axis with the recoil axis can be made. The anisotropies of the angular correlations of this experiment cannot be calculated because the mixing ratios of the gamma rays are not known. However, the energy independence may be checked.

The low energy angular correlations have the recoil axis as the symmetry axis. The symmetry axis of the higher energy measurements[20,21] is shifted away from the recoil axis. In this respect the low energy angular correlations are closer to the plane wave stripping predictions than are the higher energy measurements.

The $C^{12}(d,p_2)$ anisotropy is essentially energy independent from 2.35 MeV to 3.7 MeV. The $C^{12}(d,p_3)$ angular correlation at 2.50 MeV is as anisotropic as the higher energy measurements and the angular correlation measured at 2.35 MeV is nearly so.

In summary it might be stated that there does not appear to be any advantage to extracting reduced widths at low deuteron energies, and that the shapes of the angular distributions and angular correlations appear to support the hypothesis presented by D. H. Wilkinson.[13] Further, the angular distributions and angular correlations are remarkably energy independent. At only one resonance do both the angular distribution and the angular correlations depart drastically from stripping patterns.

APPENDICES

APPENDIX A

NEGATIVE Q STRIPPING AT LOW ENERGIES

The Butler[3] plane wave theory is based on three nuclear assumptions and one Coulomb assumption. These are the following:

1. The interaction between the deuteron and the target nucleus is ignored.
2. Once the neutron has entered the target nucleus the interaction between the proton and the neutron is ignored.
3. Elastic and inelastic deuteron scattering is ignored.
4. Coulomb effects on the incident deuteron and the emerging (or captured) proton are ignored.

Approximation 1 rules out any compound nucleus formation. This condition might be satisfied if deuterons with large impact parameters made up the major portion of the reaction. It has been stated by Butler and Hittmair[3] that $E_d \gg \frac{\hbar^2}{2m_d R_o^2}$ is a necessary condition for the nuclear assumptions to be satisfied and also that $E_d \gg \frac{Ze^2}{R_o}$ is a sufficient condition for any coulomb

effects to be small. Z is the number of protons in the nucleus, e is the charge of one electron, and R_o is the nuclear radius.

It would seem that the plane wave stripping theory would be most accurate when the deuteron energy is relatively large. Accordingly, most stripping experiments have been done at a relatively high deuteron energy. However, there appears to be one group of low bombarding energy deuteron stripping reactions where the measurements are well matched by the plane wave theory. In some cases, the agreement between the plane wave predictions and the low energy measurements is better than the agreement at higher deuteron energies. This group is that of low Q value. A striking phenomenon observed in some of these reactions is that when several excited states are reached, the low Q value states show good stripping patterns while those states with a high Q value show poor stripping patterns. These effects are more persistant in the d-p reactions than in d-n reactions.

This phenomenon was first pointed out by D. H. Wilkinson.[13] A most striking example of this phenomenon is the measurements of Sellschop.[16] Wilkinson[13] has given the following qualitative reasons for good stripping patterns.

When the Q value is high and the deuteron has only low or moderate bombarding energy, the emergent proton (in a d-p reaction for example) must receive its high momentum from the deuteron ground state wave function since there is little momentum in the bulk motion of the deuteron. In order for the proton to receive the necessary momentum from the ground state deuteron wave function, the proton and the neutron must be close to each other when the proton is stripped. Since stripping

occurs at the nuclear surface and since the proton is near the captured neutron it follows in these cases, that there is a strong likelihood that the proton will interact with the nucleus when it is stripped. The resulting angular distribution will be either badly distorted or will be the result of compound nucleus formation.

However, if the Q value is low, the proton needs little momentum and it can receive this from the deutron ground state wave function even when the neutron-proton separation is large. Proton energies of the order of the deuteron binding energy are present even when the neutron and proton are separated by the order of the relaxation length of the deutron. That the requirement that the neutron have the proper momentum at the nuclear surface can be satisfied when the n-p separation is large, can be seen by looking at the semiclassical condition:

$$\ell^2 < \frac{BE}{(h^2/mR_o^2} \qquad (1)$$

When R_o is of the order of 6 to 8 fermis, ℓ can be as large as 2. Thus, it is seen that when the Q value is low, the proton may be several fermis away from the nuclear surface when it is stripped. This inhibits nuclear distortions and compound nucleus formation and a good stripping pattern can result.

Another consideration is that when the Q value is low, the binding energy of the captured neutron is also low. It is greater than the Q value by the binding energy of the deuteron. Therefore, the neutron relaxation length is quite large in the final state and it can be relatively far away from the nucleus when it is captured. The proton is also far out from the nucleus. As

the Q value gets larger, the proton must approach the neutron and the neutron must approach the nucleus.

Yet another feature which leads to good stripping patterns for this group of reactions is that backward proton emission is inhibited by the Coulomb barrier. The Coulomb barrier for low energy deuterons inhibits a close approach of the proton to the nucleus. Since the proton must receive a large amount of momentum from the deuteron ground state wave function if it is to be emitted at a backward angle, this would imply that the proton be close to the neutron when it is stripped and this in turn imply a deeper penetration of the coulomb barrier. This is discouraged. This feature could possibly explain why the low energy-low Q value good stripping patterns are more noticeable in d-p reactions rather than d-n reactions.

Wilkinson has suggested that $E_d \approx -2Q$ should be theoptimum condition for the good low energy-low Q value stripping reaction. In this case the momentum of the stripped nucleon is about half that of the incident deuteron.

There are quantitative results which can lead to similar results as those qualitatively suggested by Wilkinson. Warburton and Chase[14] have shown that the dispersion relations derivation of the Butler stripping cross section can be used as a basis for Wilkinson's argument. According to the Feynman graph corresponding to the lowest order Born approximation for the stripping process the cross section is:[37]

$$\frac{d\sigma}{d\omega} = \left\{ \left(\frac{2J_1+1}{2J_0+1} \right) \left(\frac{3R_0 k_p}{k_d} \right) \left(\frac{2M_0}{M_1} \right) \left(\frac{\alpha}{1-\alpha r_t} \right) \left(\frac{1}{q^2+k_n^2} \right) \frac{\theta^2}{(2l+1)^2} \right\} \times$$

$$\left\{ q \left[l\, j_{l-1}(qR_0) - (l+1)\, j_l(qR_0) \right] - \left[i k_n\, j_l(qR_0) \right] \left[\frac{l h_{l-1}^{(1)}(ik_nR_0) - (l-1) h_{l+1}^{(1)}(ik_nR_0)}{h_l^{(1)}(ik_nR_0)} \right] \right\}^2 \qquad (2)$$

where:

J_1 = Spin of residual nucleus

J_o = Spin of target nucleus

R_o = Butler Radius

M_o = Target nucleus mass

M_1 = Residual nucleus mass

$\alpha = \frac{\text{Binding Energy of Deuteron}}{\hbar}$

q = the momentum transfer

r_t = Effective Triplet range

ik_n = the wave number of the captured neutron

The factor $\frac{\alpha}{1 - \alpha r_t}$ is the probability for dissociation at the first vertex.

This equation has a pole in the unphysical region $q^2 = -k_n^2$. This corresponds to a scattering angle with $|\cos \theta| > 1$. In terms of the dispersion relations approach, the Butler formula is valid when the energy denominator $(q^2 + k_n^2)$ is small compared to the energy denominator of the other poles. A stripping reaction near to this pole is generally equivalent to saying that the stripping cross section is large compared to the other processes. At the pole equation 2 is exact except for possible coulomb corrections. Butler and Hittmair[3] have shown that when the major contribution to stripping comes from high partial waves the angular distribution is not greatly affected, and if it is affected it can be corrected by a multiplicative factor. At the pole, stripping is made up of infinitely-high partial waves.

In the limit of an infinitely heavy nucleus this denominator term can be written:

$$D = \frac{\hbar^2}{2m}(q^2+k_n^2) = 3E + 2Q + \epsilon - 2(2E^2+2EQ)^{1/2}\cos\theta \qquad (3)$$

If θ is chosen equal to 0 and $\frac{\partial D}{\partial E}$ is set equal to 0, the relationship $E = -2Q$ is obtained. It will be noted that as θ gets larger D becomes larger and the distance from the pole is increased. This is a possible explanation of the breakdown of the stripping theory at large angles.

APPENDIX B

REDUCED WIDTHS

1. GENERAL DISCUSSION (Macfarlane and French - Rev. Mod. Phys. 32 (1960) 567.)

The reduced width θ^2 is a measure of the probability for the emmission of a single nucleon in the transition between two specific nuclear states. It is a useful quantity in the description of stripping as well as resonance type reactions. Stripping reactions, and hence stripping reaction reduced widths, have the advantage over resonance type reactions in that they can connect low lying levels which are inaccessible to resonance type reactions. In addition, stripping reduced widths have the further advantage of being extracted from the measured cross sections in straight-forward manner by the use of the appropriate theoretical cross sections, provided that a satisfactory theory of stripping reactions is available.

The reduced width can be considered as the product of two factors. The first factor S is the probability that in the

initial state, all but one of the nucleons will find themselves in a configuration corresponding to the final state. The spectroscopic factor S depends only upon the wave functions of the two nuclear states involved. If obtainable, the value of S would be a good means of comparing theoretical models with experimental data. The second factor θ^2_o is the probability that when an initial state is arranged in a configuration like the final state one nucleon will transfer and the final state will be formed.

$$\theta^2 = S\theta_o^2 \tag{1}$$

The plane wave Born approximation description is a useful tool for extracting reduced widths. The major difficulty with the plane wave treatment is that this theory overestimates the cross section. Hence, the reduced widths which are extracted using this treatment are too small.

The DWBA approach to extracting reduced widths appears to yield better results. The spectroscopic factor S can be calculated directly by the use of the predicted cross section. However, the DWBA optical potentials are to some extent adjustable. In addition the elastic scattering data which are necessary in the calculation of the optical potentials require longer and more difficult experiments.

In order to keep the calculations simple, the formulation and method of extracting reduced widths presented by Macfarlane and French have been utilized for this experiment. The shortcomings in calculating cross section magnitudes were assumed to be resolved by defining θ_o^2 as a strictly empirical parameter which could be evaluated by direct comparison with the experimental data.

2. PLANE WAVE REDUCED WIDTHS

The plane wave Born approximation reduced width cannot be factored into its two component probabilities, but the reduced widths in themselves might have physical significance.

The reduced width appears as a multiplicative factor in the plane wave theoretical stripping reaction cross section.

$$\frac{d\sigma}{d\omega} = 61.19 \left(\frac{M_o+1}{M_o+2}\right)^2 \left(\frac{2J_1+1}{2J_o+1}\right) \left(\frac{E}{E_d}\right)^{1/2} \{C\}^2 \sigma_{Tab}^{\ell}(x,y) R_o^3 \theta^2 \qquad (2)$$

where:

M_o = Mass of target nucleus in AMU

J_1 = Spin of residual nucleus

J_o = Spin of target nucleus

E = Kinetic Energy of stripped particle in reference frame where residual nucleus is at rest.

E_d = deuteron bombarding energy (laboratory system)

$\{C\}$ = isotropic spin coupling factor

$\sigma_{Tab}^{\ell}(x,y)$ = Cross section as listed in Lubitz tables

R_o = Butler radius

θ^2 = reduced width

For a derivation of this relationship see J. B. French, Nuclear Spectroscopy Part B, edited by F. Ajzenberg-Selove (Academic Press, New York, 1960, p. 890).

Since the reduced width is the square of a wave function, the reduced width is sensitive to the choice of the particular radius utilized in the analysis. This might explain why the reduced widths extracted from stripping reaction measurements should differ from those obtained from resonance type analysis.

However, this cannot explain the reason why the plane wave reduced widths are much too small.

The plane wave reduced widths extracted from low energy stripping data are in many cases a factor of 2 or 3 smaller than those reduced widths extracted from stripping measurements using deuterons of an energy of 7 MeV to about 15 MeV.

The reduced widths presented in Table I were obtained utilizing the method of Macfarlane and French. The method used is as follows:

a. If not already known, estimate the value of ℓ from the measured angular distributions. Also determine the spins of the various states involved.

b. Pick out a value of R_o as the cutoff radius from reference 35.

c. Calculate the quantity E by use of the relationship

$$E = \left(\frac{M_o+2}{M_o+1}\right)Q + \left(\frac{M_o}{M_o+1}\right)E_d \tag{3}$$

d. Calculate y by use of the relationship

$$y = .22R_o \left(\frac{M_o}{M_o+1}\right)(Q + 2.23)^{1/2} \tag{4}$$

e. Calculate x by use of the relationship

$$x = .22R_o\left[\frac{M_o}{M_o+2}\right]\left[2E_d+E-2(2EE_d)^{1/2}\cos\theta_{dp}\right]^{1/2} \tag{5}$$

for several values of θ_{dp} near the stripping peak

f. From Lubitz' tables obtain the values of $\sigma_{Tab}^{\ell}(x,y)$ for the values of ℓ chosen and R_o chosen

g. By adjusting ℓ and R_o find a set of $\sigma_{Tab}^{\ell}(x,y)$ which best matches the data.

h. Using the best set of $\sigma_{Tab}^{\ell}(x,y)$ calculate

$$\theta^2 = \frac{(M_o+2)^2\left(\frac{d\sigma}{d\omega}\right)(2J_o+1)}{61.19(M_o+1)(E/E_d)^2(2J_1+1)\{C\}^2\sigma_{Tab}^{\ell}(x,y)R_o^3} \qquad (6)$$

APPENDIX C

LEAST SQUARES FITTING

1. METHOD

a. GENERAL DISCUSSION

If a set of data exists which can adequately be matched by an analytical relationship, a method is needed to determine any adjustable parameters in the analytical relationship. One such means is the well known method of least squares fitting. The basic theory underlying the least squares method is well understood and will not be presented here. For the basic theory the reader is referred to Worthington and Giffner, Treatment of Experimental Data (John Wiley and Sons, Inc., New York, 1943, 238).

Many phenomenon studied in nuclear reactions are reasonably well matched by analytical relationships, and least squares fits are useful. Resonance type angular distributions

and stripping angular correlations are two examples which might be properly fitted by a least squares approach. The method of least squares was used extensively throughout the analysis of the data of this experiment. The various techniques used in the least squares fitting follow:

It is assumed that the set of data θ_i and y_i are given for $i = 1,2,\ldots N$ and it is desired to fit the function F such that

$$F(\theta_i)=y_i \text{ for } i=1,2,\ldots,N \tag{1}$$

The value of θ_i is generally assumed to be quite accurately known. It is further assumed that F has a particular form and contains the parameters $A_1, A_2,\ldots,A_n$ (i.e. the functions f is given where

$$f(A_1, A_2, \ldots, A_n, \theta_i) = F(\theta_i) \tag{2}$$

For weighted least squares fit, the parameters $A_1, A_2,\ldots, A_n$ are chosen to minimize S^2 where

$$S^2(A_1, A_2,\ldots,A_n) = \sum_{i=1}^{N}\left\{w_i^2\left[f(A_1,A_2,\ldots,A_n,\theta_i)-y_i\right]^2\right\} \tag{3}$$

where w_i^2 is the given weight for the variables θ_i and y_i. The derivation of this relationship is presented in L.D. Gates and R.N. Kubic, UTY-35 (The Babcock and Wilcox Company) June 1961. In most cases $w_i^2 = 1/\sigma_i^2$ where σ_i is the variance in the data y_i. The set of parameters $A_1, A_2, \ldots, A_n$ which minimizes S^2 is a solution of the system of equations:

$$\frac{\partial S^2}{\partial A_1}(A_1,A_2,\ldots,A_n) = 2\sum_{i=1}^{N}\left[f(A_1,A_2,\ldots,A_n,\theta_i)-y_i\right]\times \tag{4}$$

$$\left[\frac{\partial f}{\partial A_1}(A_1,A_2,\ldots,A_n,\theta_i)\right] = 0$$

$$\frac{\partial S^2}{\partial A_2}(A_1, A_2, \ldots, A_n) = 2 \sum_{i=1}^{N} \left[f(A_1, A_2, \ldots, A_n, \theta_i) - y_i\right] \times$$

$$\left[\frac{\partial f}{\partial A_2}(A_1, A_2, \ldots, A_n, \theta_i)\right] = 0$$

$$\ldots\ldots\ldots\ldots\ldots \qquad (4)$$

$$\frac{\partial S^2}{\partial A_n}(A_1, A_2, \ldots, A_n) = 2 \sum_{i=1}^{N} \left[f(A_1, A_2, \ldots, A_n, \theta_i) - y_i\right] \times$$

$$\left[\frac{\partial f}{\partial A_n}(A_1, A_2, \ldots, A_n, \theta_i)\right] = 0$$

If F is linear in the coefficients $A_1, A_2, \ldots, A_n$; this system of equations is a linear system of equations and the solution of the system for $A_1, A_2, \ldots, A_n$ is straight forward. Either the conditions $n \leq N$ and $\theta_i \neq \theta_j$ should be satisfied or the condition $n \leq$ (the number of unique values of θ) should be satisfied.

b. ITERATIVE METHODS

There are several iterative schemes for the solution of a non-linear system of equations. Because it was relatively easy to program, the Newton-Raphson method was used where an iterative method was necessary.[38] A general outline of the method follows.

An initial set $A_{1,o}, A_{2,o} \ldots A_{n,o}$ must be chosen as a first approximation to the set $A_1, A_2, \ldots, A_n$.

Then assuming differentiability and convergence S^2 is expanded by means of a Taylor's series.

$$S^2(A_1 A_2, \ldots, A_n) = \sum_{i=1}^{N} w_i{}^2 \left[f_{o,i} + \sum_{j=1}^{n} \left(\frac{\partial F}{\partial A_j}\right)_{o,i} (A_j - A_{j,o}) \right. \qquad (5)$$

$$\left. + 1/2 \sum_{j=1}^{n} \sum_{k=1}^{n} \left(\frac{\partial^2 f}{\partial A_j \partial A_k}\right)_{o,i} (A_j - A_{j,o})(A_k - A_{k,o}) + \ldots - y_i\right]^2$$

where the subscripts $_{o,i}$ indicate that the function is to be evaluated at the set $A_{1,o}, A_{2,o}, \ldots, A_{n,o}$ and θ_i.

Let us define:

$$T_o(A_1, A_2, \ldots, A_n) = \sum_{i=1}^{N} w_i^2 \left[f_{o,i} + \sum_{j=1}^{n} \left(\frac{\partial f}{\partial A_j}\right)_{o,i} (A_j - A_{j,o}) - y_i \right]^2 \qquad (6)$$

and

$$T_k(A_1, A_2, \ldots, A_n) = \sum_{i=1}^{N} w_i^2 \left[f_{k,i} + \sum_{j=1}^{n} \left(\frac{\partial f}{\partial A_j}\right)_{k,i} (A_j - A_{j,o}) - y_i \right]^2$$

Let T_o be minimized by the set $A_{1,1}; A_{2,1}; \ldots; A_{n,1}$ and T_k by the set $A_{1,k}; A_{2,k}; \ldots; A_{n,k}$)

Then:

$$\frac{\partial T_o(A_{1,1}; A_{2,1}; \ldots; A_{n,1})}{\partial A_1} = 2 \sum_{i=1}^{N} w_i^2 \left[f_{o,i} + \sum_{j=1}^{n} \left(\frac{\partial f}{\partial A_j}\right)_{o,i} (A_j - A_{j,o}) - y_i \right] \times$$

$$\left(\frac{\partial f}{\partial A_1}\right)_{o,i} = 0$$

. . . . . .

$$\frac{\partial T_o(A_{1,1}; A_{2,1}; \ldots; A_{n,1})}{\partial A_2} = 2 \sum_{i=1}^{N} w_i^2 \left[f_{o,i} + \sum_{j=1}^{n} \left(\frac{\partial f}{\partial A_j}\right)_{o,i} (A_j - A_{j,o}) - y_i \right] \times \qquad (7)$$

$$\left(\frac{\partial f}{\partial A_2}\right)_{o,i} = 0$$

. . . . . .

$$\frac{\partial T_o(A_{1,1}; A_{2,1}; \ldots; A_{n,1})}{\partial A_n} = 2 \sum_{i=1}^{N} w_i^2 \left[f_{o,i} + \sum_{j=1}^{n} \left(\frac{\partial f}{\partial A_j}\right)_{o,i} (A_j - A_{j,o}) - y_i \right] \times$$

$$\left(\frac{\partial f}{\partial A_n}\right)_{o,i} = 0$$

. . . . . .

or rewriting

$$\sum_{j=1}^{n}\left[\sum_{i=1}^{N} w_i^2 \left(\frac{\partial f}{\partial A_j}\right)_{o,i}\left(\frac{\partial f}{\partial A_1}\right)_{o,i}\right] \epsilon_{j,o} = \sum_{i=1}^{N} w_i^2 (y_i - f_{o,i})\left(\frac{\partial f}{\partial A_1}\right)_{o,i}$$

.....

$$\sum_{j=1}^{n}\left[\sum_{i=1}^{N} w_i^2 \left(\frac{\partial f}{\partial A_j}\right)_{o,i}\left(\frac{\partial f}{\partial A_2}\right)_{o,i}\right] \epsilon_{j,o} = \sum_{i=1}^{N} w_i^2 (y_i - f_{o,i})\left(\frac{\partial f}{\partial A_2}\right)_{o,i} \qquad (8)$$

.....

$$\sum_{j=1}^{n}\left[\sum_{i=1}^{N} w_i^2 \left(\frac{\partial f}{\partial A_j}\right)_{o,i}\left(\frac{\partial f}{\partial A_n}\right)_{o,i}\right] \epsilon_{j,o} = \sum_{i=1}^{N} w_i^2 (y_i - f_{o,i})\left(\frac{\partial f}{\partial A_n}\right)_{o,i}$$

where

$\epsilon_{j,o} = A_{j,1} - A_{j,o}$ for $j = 1,2,\ldots,n$

This process is repeated step by step utilizing the general equations:

$$\sum_{j=1}^{n}\left[\sum_{i=1}^{N} w_i^2 \left(\frac{\partial f}{\partial A_j}\right)_{k,i}\left(\frac{\partial f}{\partial A_1}\right)_{k,i}\right] \epsilon_{j,k} = \sum_{i=1}^{N} w_i^2 (y_i - f_{k,i})\left(\frac{\partial f}{\partial A_1}\right)_{k,i}$$

.....

$$\sum_{j=1}^{n}\left[\sum_{i=1}^{N} w_i^2 \left(\frac{\partial f}{\partial A_j}\right)_{k,i}\left(\frac{\partial f}{\partial A_2}\right)_{k,i}\right] \epsilon_{j,k} = \sum_{i=1}^{N} w_i^2 (y_i - f_{k,i})\left(\frac{\partial f}{\partial A_2}\right)_{k,i} \qquad (9)$$

.....

$$\sum_{j=1}^{n}\left[\sum_{i=1}^{N} w_i^2 \left(\frac{\partial f}{\partial A_j}\right)_{k,i}\left(\frac{\partial f}{\partial A_n}\right)_{k,i}\right] \epsilon_{j,k} = \sum_{i=1}^{N} w_i^2 (y_i - f_{k,i})\left(\frac{\partial f}{\partial A_n}\right)_{k,i}$$

where the subscripts $_{k,i}$ indicate that the function is to be evaluated at the set $A_{1,k}, A_{2,k}, \ldots, A_{n,k}$, and Θ_i. Also $\epsilon_{j,k} = A_{j,k+1} - A_{j,k}$.

This process continued until $\epsilon_{k,r} = 0$ at which point the iteration is complete.

The set $A_{1,r}; A_{2,r}; \ldots; A_{n,r}$ is our final solution. At this point the portion of equation 9 to the left of the equality is = 0. Therefore, the portion of equation 9 to the right of the equality is = 0. This right hand portion is identical to equation 4 which is what we wanted to set = 0.

Then:

$$\sum_{i=1}^{n} w_i^2 \left[f(A_{i,k};A_{2,k};\ldots;A_{n,k};\theta_i)-y_i\right]\times \left[\frac{\partial f}{\partial A_j}(A_{1,k};A_{2,k};\ldots;A_{n,k};\theta_i)\right] = 0 \text{ for } j = 1,2,\ldots,n \tag{10}$$

which is identical to equation 4. Therefore:

$$\frac{\partial S^2}{\partial A_j}(A_{1,k};A_{2,k};\ldots;A_{n,k};\theta_i) = 0 \text{ for } j = 1,2,\ldots,n \tag{11}$$

That this critical value of S^2 is a minimum value of S^2 for these particular values of the parameters $A_{1,r};A_{2,r};\ldots;A_{n,r}$ is usually apparent by the closeness of the calculated function to the experimentally measured points.

c. VARIANCE OF THE COEFFICIENTS

Once the parameters $A_1,A_2,\ldots,A_n$ are determined, it is useful to determine the possible variances in the coefficients. A scheme for the determination of the variances of the parameters $A_1,A_2,\ldots A_n$ follows:[39]

I. Using the notation of the previous section, the matrix G is defined:

$$g_{k,j} = \sum_{i=1}^{N} w_i^2 \frac{\partial f}{\partial A_k}(A_1,A_2,\ldots,A_n,\theta_i)\frac{\partial f}{\partial A_j}(A_1,A_2,\ldots,A_n,\theta_i) \tag{12}$$

The variance in the estimate of the parameter A_k is given by the equation:

$$\delta A_k = (G^{-1})_{kk} \tag{13}$$

That is the kth element along the diagonal of the inverse of the matrix G.

II. In the event that the variances of y_i are known only relatively, the method outlined above must be modified.

The weights are now equal to $\frac{1}{\xi_i^2}$ where ξ_i^2 is the relative variance and $\sigma_i^2 = \rho^2 \xi_i^2$.

Define the matrix H:

$$h_{j,k} = \sum_{i=1}^{N} \frac{1}{\xi_i^2} \frac{\partial f}{\partial A_k}(A_1, A_2, \ldots, A_n, \theta_i) \frac{\partial f}{\partial A_j}(A_1, A_2, \ldots, A_n, \theta_i) \qquad (14)$$

Now: $\delta A_k' = \rho^2 (H^{-1})_{kk}$

which is the kth element along the diagonal of the inverse of the matrix H times ρ^2.

ρ^2 is not known but can be estimated by

$$\rho^2 = \frac{S^2}{N-n} \qquad (15)$$

A rough check on the accuracy of σ_i^2 (if known absolutely) is the closeness of δA_k to $\delta A_k'$.

2. SPECIFIC EXAMPLES

The various data of this experiment were matched by the following equations:

$$F(\theta) = \sum_{p=1}^{K} A_p \cos^{(2p-2)}\theta \qquad (16)$$

$$F(\phi_\delta) = 1 + \alpha \cos^2(\phi_\delta - \phi_o') \qquad (17)$$

$$F(\phi_\delta) = 1 + A_2 \cos^2(\phi_\delta - \phi_o') + A_4 \cos^4(\phi_\delta - \phi_o') \qquad (18)$$

$$F(\phi_\delta) = 1 + b_2 \cos 2\,(\phi_\delta - \alpha 22) + b_4 \cos 4\,(\phi_\delta - \alpha 44) \qquad (19)$$

The specific relationships used in programming the least squares program and the flow chart of the program are given for each equation which was matched by the least squares method.

Case 1. If $F(\theta) = \sum_{p=1}^{K} A_p \cos^{(2p-2)}\theta$ the function F is a linear equation in A_p. Using equations 4 with n=K and

$$\frac{\partial F(\theta)}{\partial A_p} = \cos^{(2p-2)}\theta \tag{20}$$

we obtain

$$2\sum_{i=1}^{N} w_i \left[\sum_{p=1}^{K} (A_p \cos^{(2p-2)}\theta_i - y_i)(\cos^{(2p-2)}\theta_i)\right] = 0 \tag{21}$$

for all p where $p \leq N$. The set $A_1, A_2, \ldots, A_k$ may be determined by the solution of this linear set of equations. The value of K is determined by the value of k which minimizes $\frac{S^2}{N-K}$. See Figure 16.

Case 2. If $F(\phi_\gamma) = A_1 + A_2 \cos^2(\phi_\gamma - A_3)$ the function F is not linear in A_1 and equations 9 must be utalized with n=3 and

$$\frac{\partial f}{\partial A_1} = 1$$

$$\frac{\partial f}{\partial A_2} = \cos^2(\phi_\gamma - A_3) \tag{23}$$

$$\frac{\partial f}{\partial A_3} = 2A_2 \cos(\phi_\gamma - A_3)\sin(\phi_\gamma - A_3) = A_2 \sin 2(\phi_\gamma - A_3)$$

and

$$(A_1)_{k+1} = (A_1)_k + \epsilon A_{1,k}$$

$$(A_2)_{k+1} = (A_2)_k + \epsilon A_{2,k} \tag{24}$$

$$(A_3)_{k+1} = (A_3)_k + \epsilon A_{3,k}$$

Using 9, 23 and 24 we obtain:

$$\left[\sum_{i=1}^{N} w_i^2\right]\epsilon A_{1,k} + \left[\sum_{i=1}^{N} w_i^2 \cos^2(\phi_{\gamma\, i} - A_{3,k})\right]\epsilon A_{2,k} +$$

$$\left[A_{2,k}\sum_{i=1}^{N} w_i^2 \sin 2(\phi_{\gamma\, i} - A_{3,k})\right]\epsilon A_{3,k} = \sum_{i=1}^{N} w_i^2 \left\{y_i - A_{1,k} - \left[A_{2,k} \times \cos^2(\phi_{\gamma\, i} - A_{3,k})\right]\right\}$$

.....

Figure 16. Computer Method of the Least Squares Fit of

$$F(\theta) = \sum_{p=1}^{K} A_p \cos^{(2p-2)}\theta$$

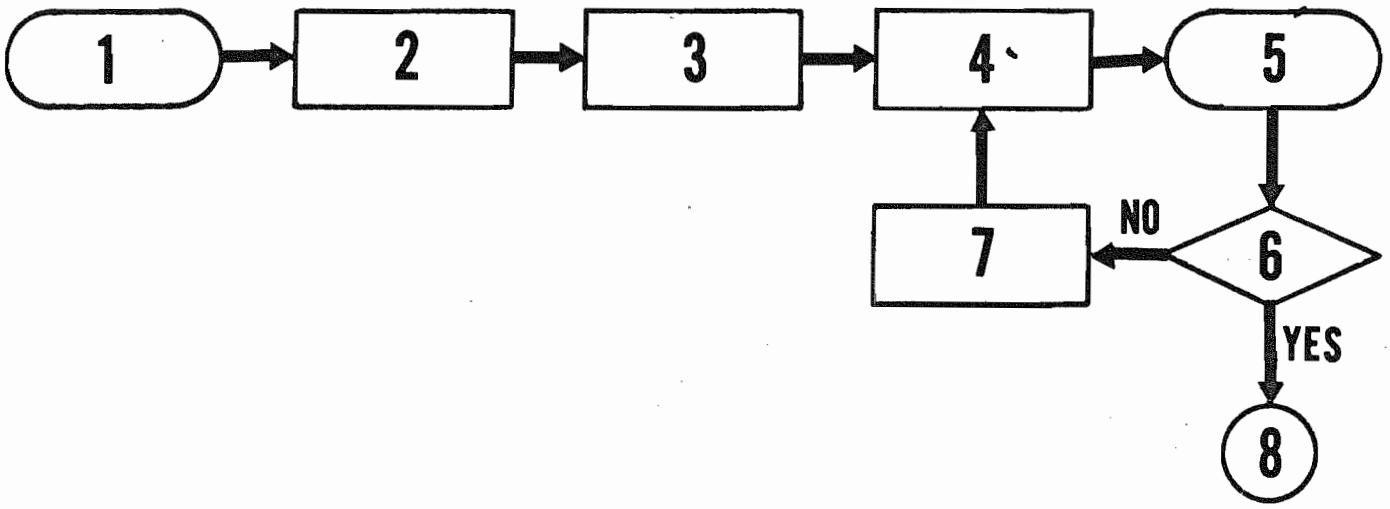

STEPS:

1 - Read y_i, w_i, θ_i, K, N

2 - Set M = 1

3 - Calculate $A_1, A_2, \ldots, A_M$ using equation 21

4 - Calculate S^2

5 - Print $\frac{S^2}{N-K}, S^2, A_1, A_2, \ldots, A_M$

6 - is $M > K$?

7 - $M = M + 1$

8 - Stop

$$\left[\sum_{i=1}^{N} w_i^2 \cos^2(\phi_{\delta i}-A_{3,k})\right] \epsilon A_{1,k} + \left[\sum_{i=1}^{N} w_i^2 \cos^4(\phi_{\delta i}-A_{3,k})\right] \chi \quad (25)$$

$$\epsilon A_{2,k} + \left[A_{2,k} \sum_{i=1}^{N} w_i^2 \sin 2(\phi_{\delta i}-A_{3,k}) \cos^2(\phi_{oi}-A_{3,k})\right] \epsilon A_{3,k}$$

$$= \sum_{i=1}^{N} w_i^2 \left[y_i - A_{1,k} - A_{2,k} \cos^2(\phi_{\delta i}-A_{3,k})\right] \cos^2(\phi_{\delta i}-A_{3,k})$$

. . . . . .

$$\left[\sum_{i=1}^{N} w_i^2 A_{2,k} \sin 2(\phi_{\delta i}-A_{3,k})\right] \epsilon A_{1,k} + \left[\sum_{i=1}^{N} w_i^2 \cos^2(\phi_{\delta i}-A_{3,k})\right] \chi$$

$$A_{2,k} \sin 2(\phi_{\delta i}-A_{3,k}) \epsilon A_{2,k} + \left[A_{2,k} \sum_{i=1}^{N} w_i^2 \sin 2(\phi_{\delta i}-A_{3,k})\right] \chi$$

$$\epsilon A_{3,k} = \sum_{i=1}^{N} w_i^2 \left[y_i - A_{1,k} - A_{2,k} \cos^2(\phi_{\delta i}-A_{3,k})\right] A_{2,k} \sin 2(\phi_{\delta i}-A_{3,k})$$

These are solved for $A_{j,k}$ by the iterative method described in the section b. See Figure 17.

Case 3. If $F(\phi_{\delta i}) = A_1 + A_2 \cos^2(\phi_\delta - A_3) + A_4 \cos^4(\phi_\delta - A_3)$ the function is not linear in A_1 and equations 9 must be utalized with n = 4. The method is identical to case 2 and will not be shown. (26)

Case 4. If $F(\phi_\delta) = A_1 + A_2 \cos 2(\phi_\delta - \alpha_{22}) + A_3 \cos 4(\phi_\delta - \alpha_{44})$ (27)

the function F is a polynoncial and is a linear system in A_i. Using equations 4 with n = 3

and

$$\frac{\partial F(\phi_\delta)}{\partial A_1} = 1$$

$$\frac{\partial F(\phi_\delta)}{\partial A_2} = \cos 2(\phi_\delta - \alpha_{22}) \quad (28)$$

Figure 17. Computer Method of the Least Squares Fit of

$$F(\phi_o) = A_1 + A_2 \cos^2(\phi_o - A_3)$$

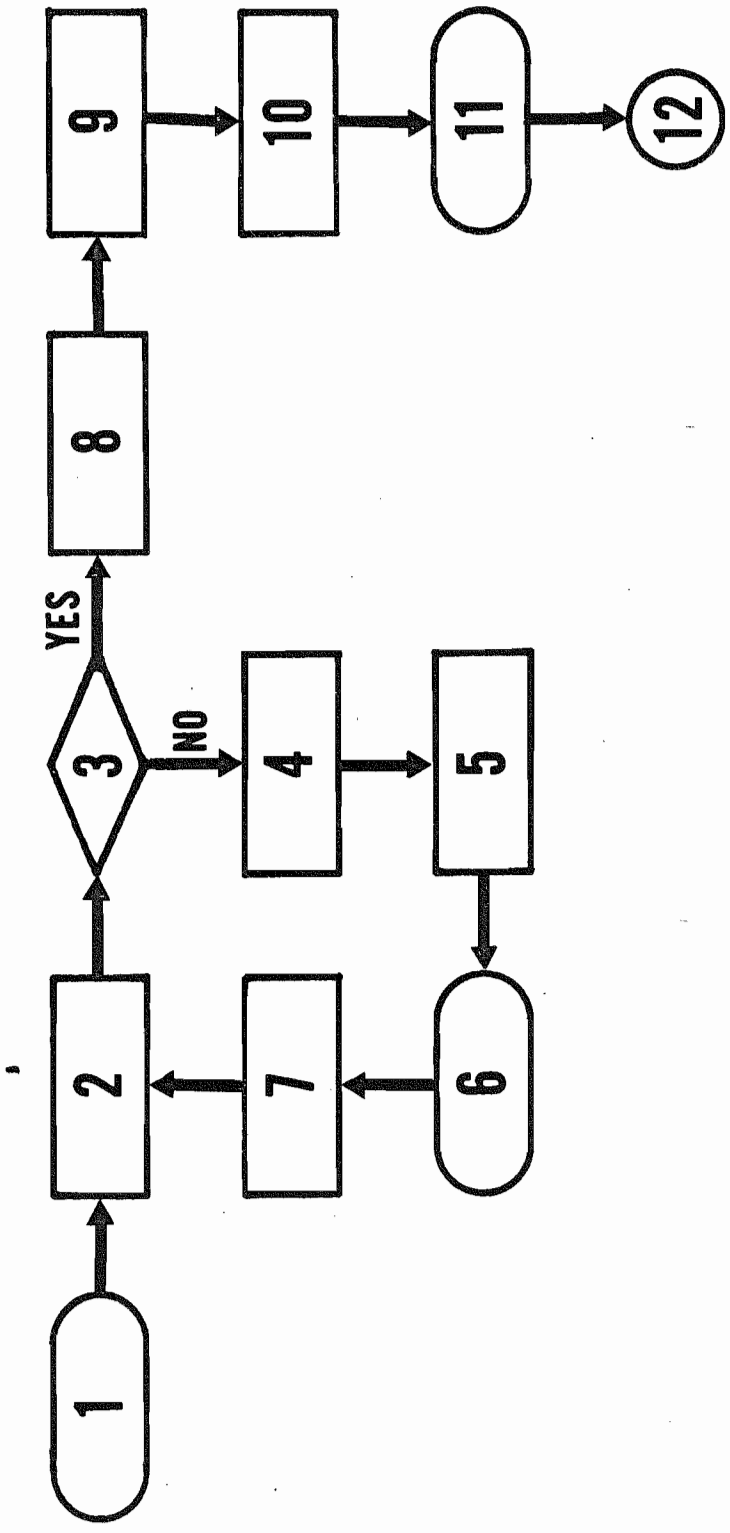
1
2
3
YES
NO
4
5
6
7
8
9
10
11
12

FLOW CHART DESCRIPTION

1. Read y_i; δ; w_i; $\emptyset_i$; $A_{1,o}$; $A_{2,o}$; and $A_{3,o}$
2. Calculate $\epsilon A_{1,k}$; $\epsilon A_{2,k}$; and $\epsilon A_{3,k}$ from equation 25
3. Is the maximum $\epsilon A_{j,k} < \delta$
4. Calculate $A_{1,k+1}$; $A_{2,k+1}$; $A_{3,k+1}$ from equation 24
5. Calculate S^2
6. Print $A_{1,k+1}$; $A_{2,k+1}$; $A_{3,k+1}$; $\epsilon A_{1,k}$; $\epsilon A_{2,k}$; $\epsilon A_{3,k}$; and S^2
7. $A_{1,k} = A_{1,k+1}$; $A_{2,k} = A_{2,k+1}$; $A_{3,k} = A_{3,k+1}$
8. Calculate final value of $A_{1,k+1}$; $A_{2,k+1}$; and $A_{3,k+1}$ using equation 24
9. Calculate S^2
10. Calculate possible errors in $A_{1,k+1}$; $A_{2,k+1}$; and $A_{3,k+1}$
11. Print $A_{1,k+1}$; $A_{2,k+1}$; $A_{3,k+1}$; S^2; possible errors in the coefficients; $\epsilon A_{1,k}$; $\epsilon A_{2,k}$; and $\epsilon A_{3,k}$.

$$\frac{\partial F(\phi_\delta)}{\partial A_3} = \cos 4(\phi_\delta - \alpha_{44})$$

we obtain

$$2\sum_{i=1}^{N} \left[A_1 + A_2\cos 2(\phi_{\delta i} - \alpha_{22}) + A_3\cos 4(\phi_{\delta i} - \alpha_{44}) - y_i\right] w_i^2 = 0$$

.....

$$2\sum_{i=1}^{N} \left[A_1 + A_2\cos 2(\phi_{\delta i} - \alpha_{22}) + A_3\cos 4(\phi_{\delta i} - \alpha_{44}) - y_i\right] w_i^2 \times$$

$$\left[\cos 2(\phi_{\delta i} - \alpha_{22})\right] = 0$$

.....

$$2\sum_{i=1}^{N} \left[A_1 + A_2\cos 2(\phi_{\delta i} - \alpha_{22}) + A_3\cos 4(\phi_{\delta i} - \alpha_{44}) - y_i\right] w_i^2 \times$$

$$\left[\cos 4(\phi_{\delta i} - \alpha_{44})\right] = 0$$

α_{22} and α_{44} must be varied in a systematic manner until a minimum in S^2 is found. See Figure 18.

Figure 18. Computer Method of the Least Squares Fit of

$$F(\phi_\delta) = A_1 + A_2\cos 2(\phi_\delta - \alpha_{22}) + A_3\cos 4(\phi_\delta - \alpha_{44})$$

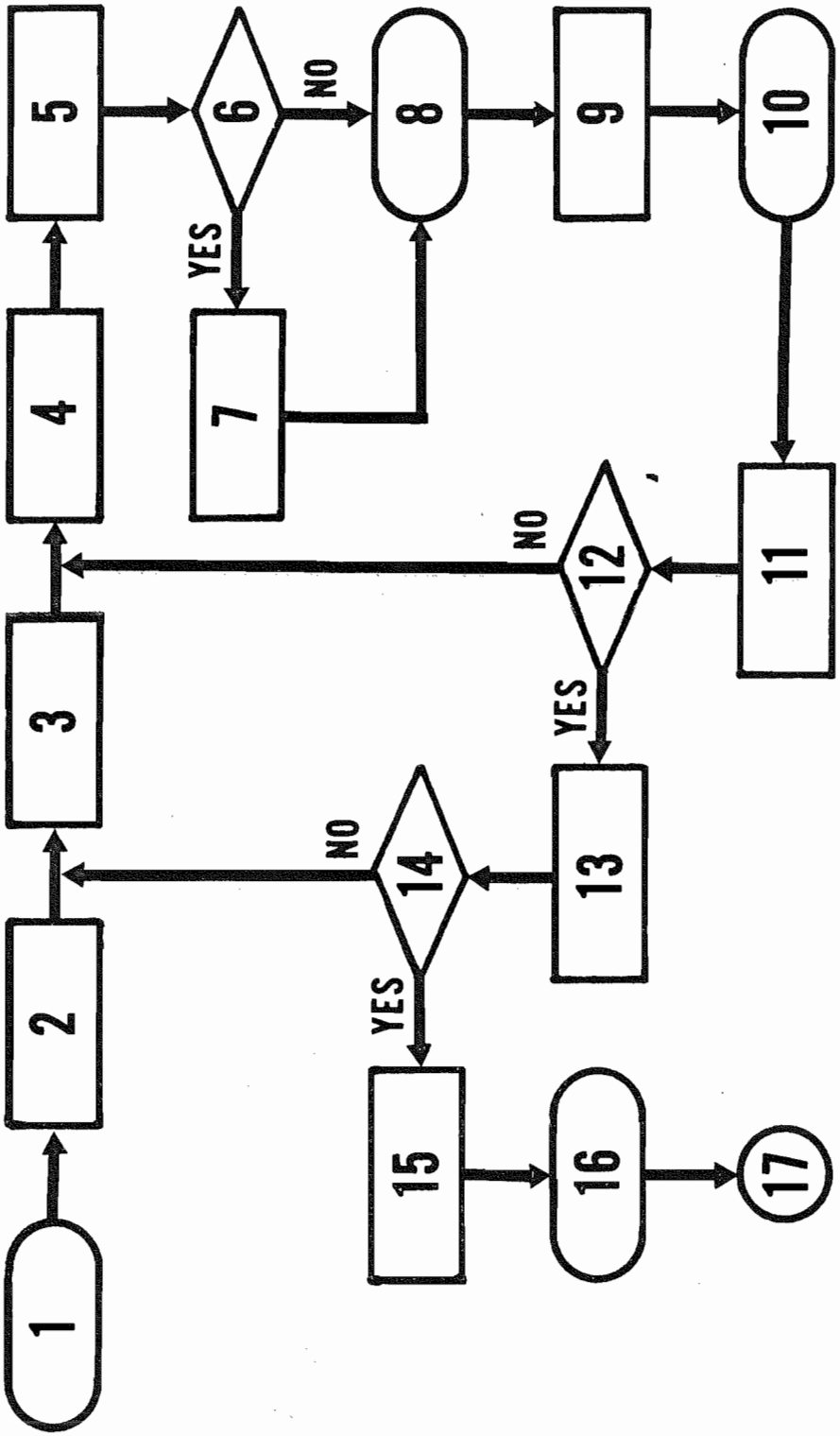
1
2
3
4
5
6
YES
NO
7
8
9
10
11
12
NO
YES
13
14
NO
YES
15
16
17

FLOW CHART DESCRIPTION

1. Read y_i; w_i; ϕ_i; $\alpha_{22,o}$; α_{22} max; $\Delta\alpha_{22}$; $\alpha_{44,o}$; α_{44} max; $\Delta\alpha_{44}$; S_o^2; N
2. $\alpha_{22} = \alpha_{22,o}$
3. $\alpha_{44} = \alpha_{44,o}$
4. Calculate A_1, A_2, and A_3 for a particular α_{22} and α_{44} using equation 29.
5. Calculate $\sum_{i=1}^{N} \frac{[y_i - F(\phi_{\gamma_i})]^2}{N-5} = S^2$
6. Is $S^2 < S_o^2$
7. $S_o^2 = S^2$, Save this set of parameters
8. Print this set of parameters and S^2
9. Calculate the possible errors in this set of parameters
10. Print the possible errors in this set of parameters
11. $\alpha_{44} = \alpha_{44} + \Delta\alpha_{44}$
12. Is $\alpha_{44} > \alpha_{44}$ max
13. $\alpha_{22} = \alpha_{22} + \Delta\alpha_{22}$
14. Is $\alpha_{22} > \alpha_{22}$ max
15. Calculate $F(\phi_{\gamma_i})$ for the set of parameters that minimizes S^2
16. Print out the set of parameters that minimizes S^2 and print out $F(\phi_{\gamma_i})$ for that set
17. Stop

LIST OF REFERENCES

LIST OF REFERENCES

1. S.T. Butler, Nuclear Stripping Reactions (John Wiley and Sons, Inc., New York, 1957).

2. A.B. Bhatia, K. Huang, R. Huby, and H.C. Newns, Phil. Mag. 43 (1952) Ser. 7, p. 485.

3. S.T. Butler, Proc. Royal Society (London), A208 (1951) 559

4. F.L. Friedman and W. Tobocman, Phys. Rev. 92 (1953) 93

5. G.R. Satchler and J.A. Spiers, Proc. Phys. Soc. (London) 65A (1952) 980.

6. G.R. Satchler, Proc. Phys. Soc. (London) 66A (1953) 1081

7. Biedenbarn, K. Boyer, and R.A. Charpie, Phys. Rev. 88 (1952) 517

8. Huby, Refai, and Satchler, Nuclear Physics 9 (1958/59) 94

9. G.R. Satchler and W. Tobocman, Phys. Rev. 118 (1960) 1566

10. L.J. Gallaher and W.B. Cheston, Phys. Rev. 88 (1952) 684

11. S.A. Cox and R.M. Williamson, Phys. Rev. 105 (1957) 1799

12. R.H. Bassell, R.M. Drisko, and G.R. Satchler, ORNL-3240 (Oak Ridge National Laboratory) Feb. 9, 1962

13. D.H. Wilkinson, Phil. Mag. 3 (Series 8) (1958) p.1185

14. E.K. Warburton and L.F. Chase, Jr., Phys. Rev., 120 (1960) 2095

15. J.P.F. Sellschop, Phys. Rev. Letters 3 (1959) 346

16. J.P.F. Sellschop, Phys. Rev. 119 (1960) 251

17. V.M. Rout, W.M. Jones, and D.G. Waters, Nuclear Physics, 34 (1962) 628

18. W.R. Gibbs and W. Tobocman, Phys. Rev. 124 (1961) 1496

19. F. Ajzenberg-Selove and T. Lauritsen, Nuclear Physics, 23 (1961) 630

20. N.R. Fletcher, D.R. Tilley and R.M. Williamson, Nuclear Physics 38 (1962) 18

21. N.R. Fletcher, Ph.D. Dissertation, Duke University (1961) unpublished.

22. M.T. McEllistrem, K.W. Jones, R. Chiba, R.A. Douglas, Phys. Rev. 104 (1956) 1008

23. T.W. Bonner, J.T. Eisinger, Alfred A. Kraus, Jr., and J.B. Marion, Phys. Rev. 101 (1956) 209

24. H.F. Chase, Jr., R.G. Johnson and E.K. Warburton, Phys. Rev. 120 (1960) 2103

25. J.M. Jeronymo, G.S. Mani, F. Picard, and A. Sadeghi, Nuclear Physics 43 (1963) 417

26. D.G. Gerke, M.A. Thesis, Duke University (1961), unpublished

27. M.T. McEllistrem, Phys. Rev. 111 (1958) 596

28. R.J. Helmer and A. Hemmendinger, Rev. Sci. Inst. 28 (1957) 649

29. Private communication, Gerke (1962)

30. J.B. Marion, K.S. Quisenberry, and C.A. Low, Jr., Phys. Rev. 120 (1960) 492

31. R.E. Warren, J.L. Powell and R.G. Herb, Rev. Sci. Inst. 18 (1947) 559

32. O. Meier, Jr., N.R. Fletcher, W.R. Wisseman and R.M. Williamson, Rev. Sci. Inst. 29 (1958) 1004

33. E.W. Hamburger, Phys. Rev. 123 (1961) 619

34. N.I. Zaika, O.F. Nemets, and M.A. Tserineo, J.E.T.P. 12 (1961) 1

35. M.H. Macfarlane and J.B. French, Rev. Mod. Phys. 32 (1960) 567

36. J.B. Garg, N.H. Gale, and J.M. Calvert, Nuclear Physics 23 (1961) 630

37. R.D. Amado, Phys. Rev. Letters 2 (1959) 399

38. A.G. Worthington and J. Geffner, Treatment of Experimental Data (John Wiley and Sons, Inc., New York, 1943)

39. P. Czeffra and M.J. Moravcsik, UCRL-8523, (University of California Lawrence Radiation Laboratory) 1958

BIOGRAPHY

Thomas Sidney Katman

Born:

April 17, 1934
Philadelphia, Pennsylvania

Education:

University of Delaware, 1952-1956
B.S. (Physics), 1956

Duke University, 1956-1964
Teaching Assistant, 1956-1957
Research Assistant, 1957-1962

Publications:

T.S. Katman and R.M. Williamson, "Na^{23} and $Al^{27}(\alpha, n)$ Reaction Energies", Bull. Am. Phys. Soc. II, 4, 286 (1960)

R.M. Williamson, T.S. Katman, and B.S. Burton, "F^{19}, Na^{23}, and $Al^{27}(\alpha, n)$ Reactions", Phys. Rev., 117, 1325 (1960)

T.S. Katman, D.R. Tilley, R.M. Williamson, D.G. Gerke, J.M. Lacambra and J.R. Sawers, "Proton-γ Angular Correlations in the $C^{12}(d,p)$ C^{13} Reaction at Low Energies", Bull. Am. Phys. Soc. II, 8, 7 (1963)

Societies:

American Physical Society
Sigma Pi Sigma